

STUDIES OF A TRYPANOSOMAL SULFHYDRYL OXIDASE

by

Jennifer Marie Kurek

A thesis submitted to the Faculty of the University of Delaware in partial fulfillment of the requirements for the degree of Master of Science in Chemistry and Biochemistry

Spring 2014

© 2014 Jennifer Kurek
All Rights Reserved

UMI Number: 1562394

All rights reserved

INFORMATION TO ALL USERS

The quality of this reproduction is dependent upon the quality of the copy submitted.

In the unlikely event that the author did not send a complete manuscript and there are missing pages, these will be noted. Also, if material had to be removed, a note will indicate the deletion.



UMI 1562394

Published by ProQuest LLC (2014). Copyright in the Dissertation held by the Author.

Microform Edition © ProQuest LLC.

All rights reserved. This work is protected against unauthorized copying under Title 17, United States Code



ProQuest LLC.
789 East Eisenhower Parkway
P.O. Box 1346
Ann Arbor, MI 48106 - 1346

STUDIES OF A TRYPANOSOMAL SULFHYDRYL OXIDASE

by

Jennifer Marie Kurek

Approved: _____
Colin Thorpe, Ph.D.
Professor in charge of thesis on behalf of the Advisory Committee

Approved: _____
Murray Johnston, Ph.D.
Chair of the Department of Chemistry and Biochemistry

Approved: _____
George Watson, Ph.D.
Dean of the College of Arts and Sciences

Approved: _____
James G. Richards, Ph.D.
Vice Provost for Graduate and Professional Education

PREFACE

Publications from which figures were adapted are given proper credit in the respective figure captions. Publications from which figures were taken are used with permission from the publisher (see appendix) and are also credited in the respective figure captions. Unpublished data that is not my own is credited in the text to the individual who produced the data. Unpublished figures that are not my own are credited beside the figure to the individual who produced the figure.

I would like to give my most heartfelt thanks to my advisor, Dr. Colin Thorpe, for his wisdom, advice, and understanding throughout my graduate career. His guidance was both generous and indispensable.

I would like to thank the members of my Committee, Dr. Brian Bahnson, Dr. Jung-Youn Lee, and Dr. Mary Watson for their willingness to foster my success as a graduate student and expand my knowledge as a biochemist. Their dedication and individual expertise were vital to my growth and achievement.

I would like to thank all present and past members of the Thorpe laboratory for their guidance, support and most importantly, their companionship. I have learned so much from each of you and wish you all the best in your future endeavors. I would especially like to thank Benjamin Israel for his mentorship upon my arrival to the laboratory.

I would like to thank my mother and my father for their unconditional love, encouragement, and strength throughout not only my graduate career but throughout my life. I dedicate this work and all that I do to you.

TABLE OF CONTENTS

LIST OF FIGURES	vi
ABSTRACT	xi
Chapter	
1 OXIDATIVE PROTEIN FOLDING.....	1
1.1 Disulfide Bond Formation.....	1
1.2 Quiescin Sulphydryl Oxidase (QSOX) Protein Family	3
1.3 ERV/ALR Sulphydryl Oxidase Protein Family	8
1.4 Ero1 Family of Sulphydryl Oxidases.....	16
2 TRYPANOSOMA.....	18
2.1 Physiology	18
2.2 African Sleeping Sickness.....	20
2.2.1 Symptoms	20
2.2.2 Statistics.....	21
2.2.3 Diagnosis and Treatment.....	21
2.2.4 Trypanosome Variable Surface Glycoproteins and the Host Immune System.....	23
2.2.5 Sulphydryl Oxidases Present in Trypanosomes.....	26
3 OXIDATIVE FOLDING AND THE DISULFIDE RELAY SYSTEM IN THE INTERMEMBRANE SPACE (IMS) OF MITOCHONDRIA IN MOST EUKARYOTES	29
3.1 Mitochondria	29
3.2 The Intermembrane Space and the Mitochondrial Intermembrane Space Assembly Pathway.....	29
3.3 Substrates of the Intermembrane Space Assembly Pathway.....	30
4 OXIDATIVE FOLDING AND THE DISULFIDE RELAY SYSTEM IN THE INTERMEMBRANE SPACE (IMS) OF THE MITOCHONDRION IN TRYPANOSOMES.....	33

5	PREVIOUS WORK WITH QUIESCIN SULFHYDRYL OXIDASE 2 AND TRYPANOSOMA BRUCEI AUGMENTER OF LIVER REGENERATION	38
5.1	Quiescin Sulphydryl Oxidase 2.....	38
5.2	Trypanosomal Augmenter of Liver Regeneration.....	38
6	CURRENT WORK WITH TRYPANOSOMA BRUCEI AUGMENTER OF LIVER REGENERATION	46
6.1	Protein Purity Improvement Using Inclusion Body Purification	46
6.2	Circumventing Trypanosomal ALR's Aggregation through Generation of Fusion Proteins.....	52
6.3	Investigation of Arsenical Inhibition by Trypanosomal ALR.....	59
6.4	Side Projects with Trypanosomal ALR.....	64
	REFERENCES	65
Appendix		
	PERMISSION LETTERS	72

LIST OF FIGURES

Figure 1:	The two steps of oxidative protein folding. Figure adapted from (Thorpe, 2013).....	2
Figure 2:	Disulfide bond formation in the ER. The top panel shows The QSOX/PDI pathway of disulfide bond formation in the ER. The bottom panel shows the classic view of disulfide bond formation involving PDI and Ero1/Erv2. Figure adapted from (Thorpe, 2013).	4
Figure 3:	The domain structure and flow of electrons during the catalytic oxidation of a substrate by QSOX. Redox-active CXXC motifs are shown as yellow bars. Figure taken from (Coddling et al., 2012) with permission from the publisher.	6
Figure 4:	Steric requirements of a QSOX. The attacking thiolate must be linear with the receiving disulfide bond. Figure taken from (Coddling et al., 2012) with permission from the publisher.	6
Figure 5:	Reaction scheme for a typical FAD dependent sulfhydryl oxidase. A dithiol substrate (or distal disulfide) is represented by a wavy line. The isoalloxazine ring of the FAD cofactor and the proximal disulfide are included in the boxes. The second cysteine residue of the proximal disulfide is referred to as the “charge-transfer” thiol, as it forms a charge-transfer complex with the flavin cofactor (e.g. box E). The first cysteine forms mixed disulfides with the substrate (or with the distal disulfide) (box C) and so is referred to as the “interchange” cysteine. Figure adapted from (Kodali and Thorpe, 2010a).....	7

Figure 6:	<p>Panel A shows variability in the location of the shuttle disulfide in different organisms, along with where the enzyme is found. The ERV domain is shown in pink and the FAD cofactor is shown in yellow. The proximal CXXC motif is located within the ERV domain and is shown in red. The distal, or shuttle, CXXC motif is located within either the N- or C-terminal extension and is shown in gray. Intracellular locations of the enzymes are in parentheses. Figure adapted from (Thorpe, 2013). Panel B shows proximal CXXC motif and shuttle CXnC motif communication of a typical single domain ERV/ALR protein. The shuttle disulfide is located on a flexible loop of the protein, at either the N- or C- terminus. Figure adapted from (Vitu et al., 2006).</p>	10
Figure 7:	<p>Electron flow during catalysis by Erv2p is represented sequentially by arrows. The two homodimers of the protein are shown in blue and gray. The FAD cofactor is represented in ball and stick form and both the shuttle and proximal CXXC motifs are yellow sticks. In every case studied, the wild-type protein is a homodimer with reducing equivalents from the substrate being passed from the shuttle disulfide of one subunit to the proximal disulfide in the second subunit. Figure taken from (Thorpe and Coppock, 2007) with permission from the publisher.</p>	12
Figure 8:	<p>Oxidative folding in the IMS. Either oxygen or cytochrome c reoxidize ALR/Erv1p. Figure taken from (Daithankar et al., 2009) with permission from the publisher.</p>	13
Figure 9:	<p>Depiction of R194 H-bond participation in human sfALR and the R194H mutant. Panel A shows that R194 forms H-bonds with the 2' OH of the ribityl moiety of FAD, its own main chain peptide carbonyl, and the main chain carbonyl oxygen contributed by C95 of the other (green) subunit. Panel B shows the interactions of the R194H mutant. Figure taken from (Daithankar et al., 2010) with permission from the publisher.</p>	15
Figure 10:	<p>Crystal structure of Ero1 in yeast. The crystal structure of yeast Ero1p. N-terminus is blue. C-terminus is red. The proximal disulfide (yellow spheres) is next to the FAD isoalloxazine ring (yellow ball and stick). The shuttle Cx4C disulfide (orange spheres) is located on a mobile loop (red). Disulfide bonds shown in gold sticks are regulators of oxidase activity. Their reduction initiates the oxidation of reduced PDI by the enzyme. N- and C-termini are depicted in blue and red respectively. Figure adapted from (Thorpe, 2013).</p>	17

Figure 11: ClustalW2 multiple sequence alignment of human lfALR, yeast Erv1, and TbALR. Cysteine residues are highlighted in pink.	27
Figure 12: Domain representation of yeast Erv1, human lfALR, and TbALR. FAD is represented by yellow hexagons. Cysteines are represented by yellow bars. The ERV/ALR domain is green, while the rest of the protein is blue.	27
Figure 13: Crystal structure of yeast Erv1 shows the redox-active proximal (C130–C133) and distal (C30-C33) disulfides and the structural disulfide (C171–C188) depicted as yellow spheres. The FAD is depicted in ball and stick form.	28
Figure 14: SDS-PAGE gel of soluble WT TbALR after Ni-NTA chromatography. Lane 1 is the protein marker (molecular weights in yellow; kDa). The red arrow indicates the TbALR proteolysis contaminant.	40
Figure 15: SDS-PAGE gel of TbALR' after inclusion body purification and the novel refolding method. Lane 1 is the protein marker (molecular weights in yellow; kDa). Lanes 2 and 3 are under reducing and non-reducing conditions, respectively. The red arrow indicates the TbALR proteolysis contaminant.	42
Figure 16: SDS-PAGE gel of TbALR' following lysis under denaturing and reducing conditions. Lane 1 is the protein marker (molecular weights on the left; kDa) Lane 3 is under reducing conditions. Lane 5 is under non-reducing conditions. The red arrow indicates the TbALR' proteolysis contaminant.	44
Figure 17: Catalytic parameters for TbALR' (' indicates C14S mutant). Panel A. pH profile of TbALR' with 10 mM DTT shows an optimal pH around 9.0. Panel B. Michaelis-Menten parameters for TbALR' using DTT as a substrate in oxygen electrode assay.	45
Figure 18: Expression gel of TbALR'. IPTG induction, BL21*DE3 cells, 37 °C. Lane 1 (M) is the marker. Molecular weights of the marker are in kDa. Lane 2 (Pre) is the pre-induced sample. Lanes 4-6 are hours 2-6 post induction. TbALR' is indicated by a blue arrow.	47

Figure 19:	TbALR' post cell lysis, post pellet solubilization, and post protein renaturation. Lane 1 (M) is the marker. Molecular weights of the marker are in kDa. Lane 2 (PLS) is the soluble fraction post cell lysis. Lane 3 (PLP) is the insoluble fraction post cell lysis. Lane 4 (PSS) is the soluble fraction post denaturing and reducing. Lane 5 (PSP) is the insoluble fraction post denaturing and reducing. Lane 6 (PRS) is the solution after being renatured. PLS: Post Lysis Supernatant; PLP: Post Lysis Pellet; PSS: Post Solubilizing Supernatant; PSP: Post Solubilizing Pellet; PRS: Post Renaturing Supernatant. TbALR' is indicated by a blue arrow.	48
Figure 20:	Michaelis-Menten parameters for TbALR' using DTT as a substrate in an oxygen electrode assay. The buffer used was 50 mM Tris containing 1 mM EDTA and 20% glycerol, pH 8.5.....	51
Figure 21:	Nucleic acid sequence of Trx: TbALR fusion protein. The 6X His Tag is in green. The thioredoxin domain is in magenta. The TEV protease cleavage site is in lilac. TbALR is in cyan. The cysteines of TbALR are highlighted in yellow. The C14 position (mutated to a serine in experiments) is highlighted in magenta.....	53
Figure 22:	Expression gel of Trx: TbALR'. IPTG induction, BL21*DE3 cells, 37 °C/ 15 °C. Lane 1 is the pre-induced sample. Lanes 2, 4, and 5 are 1, 3, and 5 hours post induction, respectively. Lane 3 (M) is the marker. Molecular weights of the marker are in kDa. Trx: TbALR' is indicated by a blue arrow.	54
Figure 23:	IMAC purification gel of Trx: TbALR' using an Ni-IDA column. Lane 1 (PLP) is the post-lysis pellet. Lane 2 (PLS) is the post lysis supernatant. Lane 3 (M) is the marker. Molecular weights of the marker are in kDa. Lane 4 (FT) is the flow through. Lanes 5 (W1) and 6 (W2) are buffer washes. Lanes 7-10 are elution fractions with 200 and 500 mM imidazole concentrations. PLP: Post Lysis Pellet; PLS: Post Lysis Supernatant; FT: Flow Through; W: Wash. Trx: TbALR' is indicated by a blue arrow.	55
Figure 24:	TEV Protease and Trx: TbALR' separation attempt via IMAC using an Ni-IDA column. Lane 1 (TEV) is TEV protease alone. Lane 2 (Post TEV) is Trx: TbALR' post incubation with TEV protease. Lane 3 (M) is the marker. Molecular weights of the marker are in kDa. Lane 4 (Pre TEV) is Trx: TbALR' before incubation with TEV protease. Lane 5 (FT) is the flow through. FT: Flow Through. Trx: TbALR' is indicated by a green dot. TEV protease is indicated by a blue dot. Thioredoxin is indicated by a red dot.	57

Figure 25:	TEV Protease and Trx: TbALR' separation attempt via size exclusion chromatography and ion exchange chromatography. Lane 1 (M) is the marker. Molecular weights of the marker are in kDa. Lane 2 (Post TEV) is Trx: TbALR' post incubation with TEV protease. Lane 3 (Post S.E.) is Trx: TbALR' after size exclusion chromatography was performed. Lane 4 (Post I.E. pH 8) is Trx: TbALR' after anion exchange chromatography was performed. Lane 5 (TEV) is TEV protease alone. Lane 6 (Post I.E. pH 8) is Trx: TbALR' after cation exchange chromatography was performed. S.E.: Size Exclusion; I.E.: Ion Exchange. Trx: TbALR' is indicated by a green dot. TEV protease is indicated by a blue dot. Thioredoxin is indicated by a red dot.	58
Figure 26:	Michaelis-Menten parameters for Trx: TbALR' using DTT as a substrate in an oxygen electrode assay. The buffer used was 50 mM Tris containing 1 mM EDTA and 20% glycerol, pH 8.5.	59
Figure 27:	Coordination of thiols. Panel A shows alkyl- or aryl- arsenicals. Panel B depicts arsonous acid.	60
Figure 28:	Representative bead of the arsenic resin designed and synthesized by Aparna Sapa.	62
Figure 29:	Crithidia fasciculata lysate incubated in the presence or absence of TCEP with arsenic resin. M: Marker; FT: Flow Through; W: Wash; β : β -Mercaptoethanol; D: Dithiothreitol. Molecular weights of the marker are in kDa.	63

ABSTRACT

Trypanosomal augmenter of liver regeneration (ALR) is a fascinating protein operating in the intermembrane space of mitochondria. It is a key participant in the disulfide relay system of the mitochondrial intermembrane space assembly (MIA) pathway where it helps to correctly fold proteins imported into the intermembrane space. The MIA pathway in most eukaryotes is initiated by Mia40, the first protein in the disulfide relay system. The role ALR plays in the MIA pathway in trypanosomes is unknown, as they lack Mia40 altogether. Does ALR perform the function of Mia40 and act alone, or is there a partnership with a Mia40 homolog not yet identified? Trypanosomal ALR proved to be an extremely problematic protein to purify and characterize due to its tendency to aggregate. Following an introduction to oxidative protein folding, sulfhydryl oxidases, and the parasite, *Trypanosoma brucei*, this thesis addresses the problem of aggregation and the paths taken to circumvent it. Following a serendipitous discovery involving arsenic from the 1900s, possible therapeutics against the African Sleeping Sickness targeting the protein were also explored, along with kinetic and structural aspects of the protein.

Chapter 1

OXIDATIVE PROTEIN FOLDING

1.1 Disulfide Bond Formation

Disulfide bonds are one of the most well-known forms of post-translational modification in the cell. They are involved in a number of cellular processes, from stabilizing protein structure to regulating redox pathways. Though the many roles disulfide bonds play in cells do not constitute new information, the mechanism behind their formation has remained unknown in higher eukaryotic organisms (1-6).

The process by which disulfide bonds are generated in a protein is called oxidative protein folding and involves two steps depicted in Figure 1. The first step involves the formation of a covalent sulfur-sulfur bond through the removal of two reducing equivalents – one per each cysteine residue involved in the bond. The second step involves isomerization of any mispaired disulfide bonds introduced in the first phase of catalysis. This latter reaction is catalyzed by a member of the protein disulfide isomerase (PDI) family (4, 5).

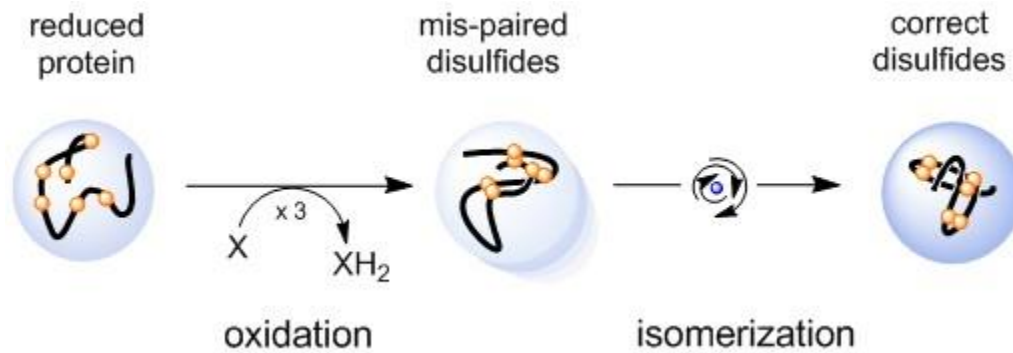


Figure 1: The two steps of oxidative protein folding. Figure adapted from (Thorpe, 2013).

Disulfide bonds are formed in multiple locations in the eukaryotic cell – namely the secretory system, which is comprised of the endoplasmic reticulum (ER), Golgi, and post-Golgi compartments (5). The intermembrane space (IMS) of the mitochondria also has its own disulfide formation pathway, known as the disulfide relay system, or MIA (mitochondrial intermembrane space assembly) pathway (7). It is this system of disulfide bond formation that is the focus of my research. It is important to note that the locations of disulfide formation in the cell are comparatively oxidizing environments, compared to the normal cytosol, which is quite reducing. Disulfide bond formation is not limited to the cell interior however, and also occurs extracellularly: at the cell surface and within the extracellular matrix (ECM) (4, 5).

How are disulfide bonds formed? Many of these locations in the cell utilize a class of enzymes known as sulfhydryl oxidases to catalyze disulfide bond formation. Disulfide bond generation arising from sulfhydryl oxidase activity can be described by the following reaction:



The well documented sulfhydryl oxidases utilize a flavin cofactor, flavin adenine dinucleotide (FAD) and a redox active CXXC motif proximal to the flavin to carry out catalysis (5).

1.2 Quiescin Sulfhydryl Oxidase (QSOX) Protein Family

The first member of this flavin-dependent sulfhydryl oxidase family was discovered through purification of rat seminal vesicle proteins. The 66 kDa protein was observed as a yellow band during chromatography and showed FAD-dependent oxidase activity when in the presence of mono- and dithiol substrates (5, 8). The similarity between this sulfhydryl oxidase and a human growth factor, Quiescin Q6, was subsequently discovered (5, 9, 10) – thus birthing the quiescin sulfhydryl oxidase (QSOX) protein family (5, 11).

The QSOX/PDI pathway of disulfide bond formation in the ER (Figure 2, top panel) is quite different than the classic view of disulfide bond formation involving PDI and Ero1/Erv2 (yeast) (Figure 2, bottom panel). In the Ero1 pathway, PDI inserts the disulfide bonds, becomes re-oxidized by Ero1, and then intervenes a second time to isomerize the protein (5, 12, 13). In the QSOX pathway, QSOX directly inserts disulfide bonds into the protein while PDI isomerizes any mispairings (5, 11-13). Both pathways involve the consumption of oxygen and the generation of hydrogen peroxide as reducing equivalents are passed from the substrate to molecular oxygen (5).

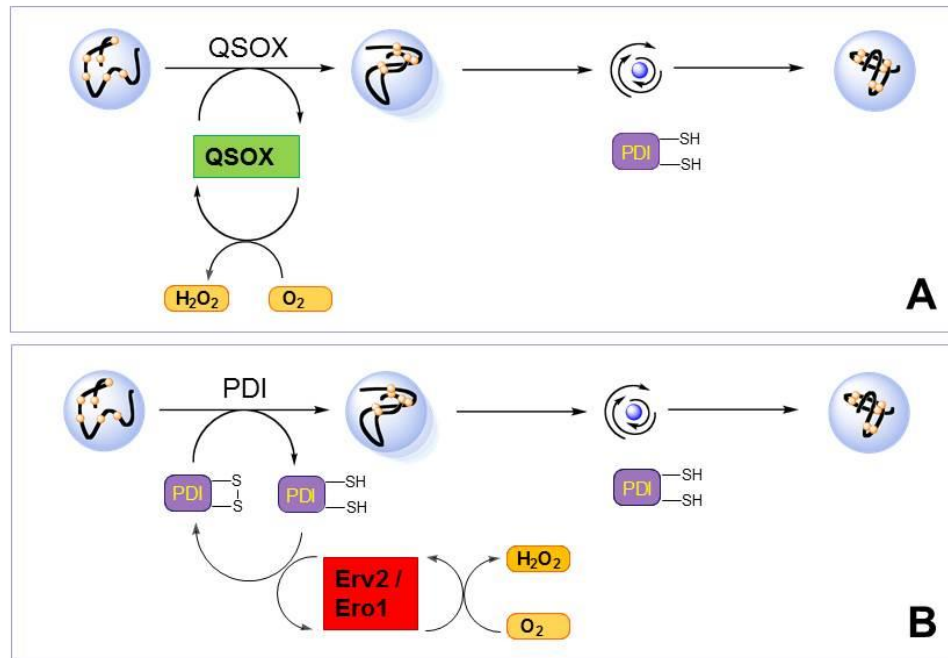


Figure 2: Disulfide bond formation in the ER. The top panel shows The QSOX/PDI pathway of disulfide bond formation in the ER. The bottom panel shows the classic view of disulfide bond formation involving PDI and Ero1/Erv2. Figure adapted from (Thorpe, 2013).

How does QSOX perform the same oxidizing activity as both PDI and Ero1 combined? The answer lies in the domain structure of QSOX – an ancient fusion of both Trx (thioredoxin) and ERV (Essential for Respiration and Vegetative Growth) domains. QSOXs are found in all multicellular organisms studied to date (14). They contain either one (algae, plants, and protists) (4, 5) or two (metazoan) Trx domains, a helix rich region (HRR) of about 100 amino acids, and an ERV domain (5, 16). The domain structures of QSOX are depicted in Figure 3. It was the discovery of the ERV

domain in QSOX that led to the discovery that the yeast growth factors, Erv1p and Erv2p, were also FAD dependent sulfhydryl oxidases. The domain responsible for FAD binding was the ERV domain (4, 5).

QSOX combines one redox active Trx domain with two, four helix bundle domains (HRR-ERV) – the latter reminiscent of the homodimeric structure of Erv2p. Together, these domains shuttle reducing equivalents from the substrate protein to oxygen, generating oxidized protein and hydrogen peroxide at the end of the catalytic process (Figure 3). QSOXs prefer reduced and unfolded protein substrates (5, 17, 18) and all contain 3 conserved CXXC motifs (distal disulfide in the redox active Trx domain, proximal disulfide in communication with the FAD cofactor, and redox inactive disulfide near the C-terminus of the ERV domain) (5, 19-21). QSOX substrates approach the distal disulfide first and interact via a mixed disulfide between the substrate protein (attacking thiolate) and the first sulfur of the distal disulfide pair. The mixed disulfide is then resolved via a second thiolate attack from the substrate protein, producing oxidized protein and reduced Trx domain. It is thus easily understandable that monothiols are not strong substrates as there is no second sulfur locally available to attack and resolve the mixed disulfide (5).

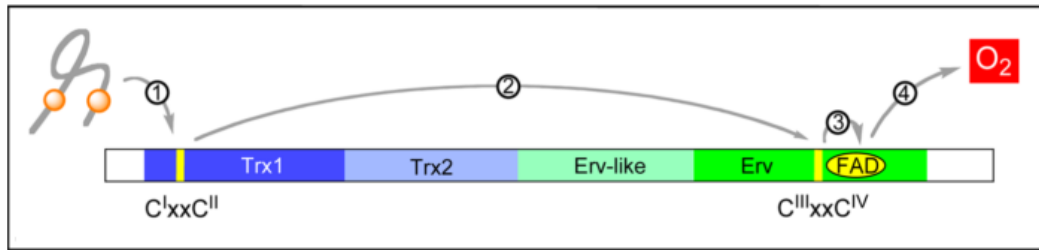


Figure 3: The domain structure and flow of electrons during the catalytic oxidation of a substrate by QSOX. Redox-active CXXC motifs are shown as yellow bars. Figure taken from (Coddling et al., 2012) with permission from the publisher.

The QSOX mechanism does have steric limitations. Optimally, the attacking thiolate must be linear with the receiving disulfide bond (5, 17), as shown in Figure 4. This is why bulky proteins (i.e. well folded proteins) are poor substrates (5, 17, 22). QSOX (in nanomolar concentrations), along with PDI (micromolar concentrations) can facilitate oxidative protein folding of a variety of reduced and unfolded proteins to their native forms (5, 23), with a catalytic upper limit in the range of 600-2000 inserted disulfides per minute (5, 18, 20, 21, 24).

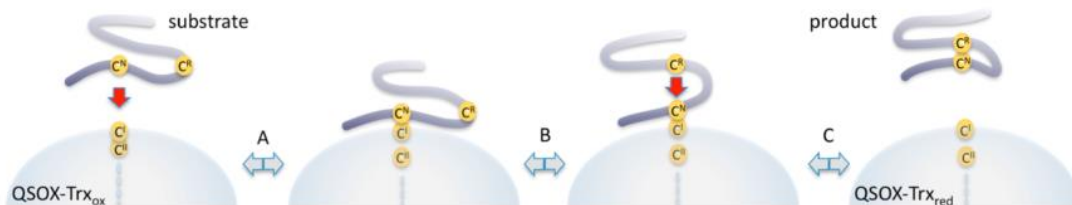


Figure 4: Steric requirements of a QSOX. The attacking thiolate must be linear with the receiving disulfide bond. Figure taken from (Coddling et al., 2012) with permission from the publisher.

When the first or second sulfur of the distal disulfide is mutated, the catalytic power of the enzyme is severely hampered because the substrate now can only interact with the enzyme via its proximal disulfide (housed in the ERV domain). This additional disulfide is an important player in the activity of the QSOX enzymes. A minimal reaction scheme for a general sulfhydryl oxidase is presented in Figure 5. The ERV family enzymes, as well as the Ero1 family enzymes, also utilize distal disulfides to “shuttle” reducing equivalents to the proximal disulfide near the FAD cofactor (5, 8, 20, 22, 25).

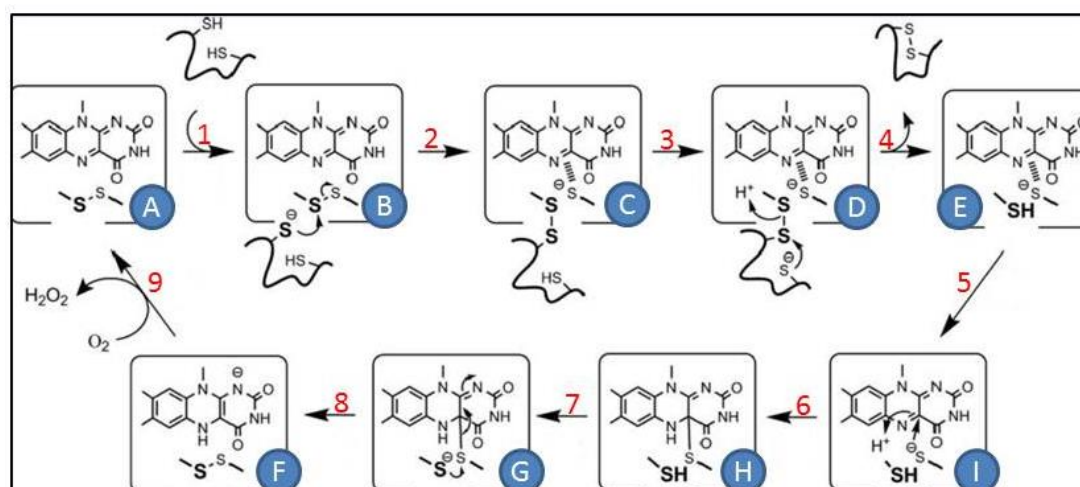


Figure 5: Reaction scheme for a typical FAD dependent sulfhydryl oxidase. A dithiol substrate (or distal disulfide) is represented by a wavy line. The isoalloxazine ring of the FAD cofactor and the proximal disulfide are included in the boxes. The second cysteine residue of the proximal disulfide is referred to as the “charge-transfer” thiol, as it forms a charge-transfer complex with the flavin cofactor (e.g. box E). The first cysteine forms mixed disulfides with the substrate (or with the distal disulfide) (box C) and so is referred to as the “interchange” cysteine. Figure adapted from (Kodali and Thorpe, 2010a).

Where is QSOX located in the cell? In mammalian cells, there are two forms of QSOX: QSOX1 and QSOX2. QSOX1 is plentiful in tissues that are burdened by a heavy secretory load. Intracellular QSOX is located in the ER, Golgi, secretory vesicles and at nuclear/plasma membranes (5). QSOX1 can be anchored to the cell surface via a C-terminal helix that spans the membrane. If this anchor is absent (via expression of a splice variant or following protease degradation), the short form is secreted in body fluids like tears (5, 25) and blood (5, 26). Roles for secreted QSOX could include disulfide bond formation for instances when the task is too large to be completed within the confines of the cell. External QSOX could act as a microbial agent (8) or facilitate cell: cell signaling (5, 27). Interestingly, QSOX is present (and overexpressed) in prostate (5, 28) and pancreatic cancer cells (5, 29).

QSOX2 exists in generally lower concentrations in a variety of tissues and is still inadequately understood. It was this enzyme that began my graduate research career (more later).

1.3 ERV/ALR Sulfhydryl Oxidase Protein Family

The ERV domain present in the QSOX family of sulfhydryl oxidases is also present in single domain, homodimeric enzymes of the same basic function. These ERV family proteins are found in the cytosol, ER and IMS. As mentioned earlier, many of these enzymes contain a distal disulfide, capable of passing reducing equivalents from the substrate to the proximal disulfide that communicates with the FAD (5). These distal, or shuttle, disulfides are present within either the N- (fungi and mammals) or C-terminus (plants) (30) of the protein. It is important to note that the spacing between the two cysteine residues of the shuttle disulfide as well as the distance between the ERV/ALR domain and the first cysteine of the shuttle differs

from species to species (30). Figure 6, Panel A depicts the variability in the location of the shuttle disulfide in different organisms, along with their cellular locales. Panel B shows the communication between redox active cysteines in most ERV/ALR single domain proteins.

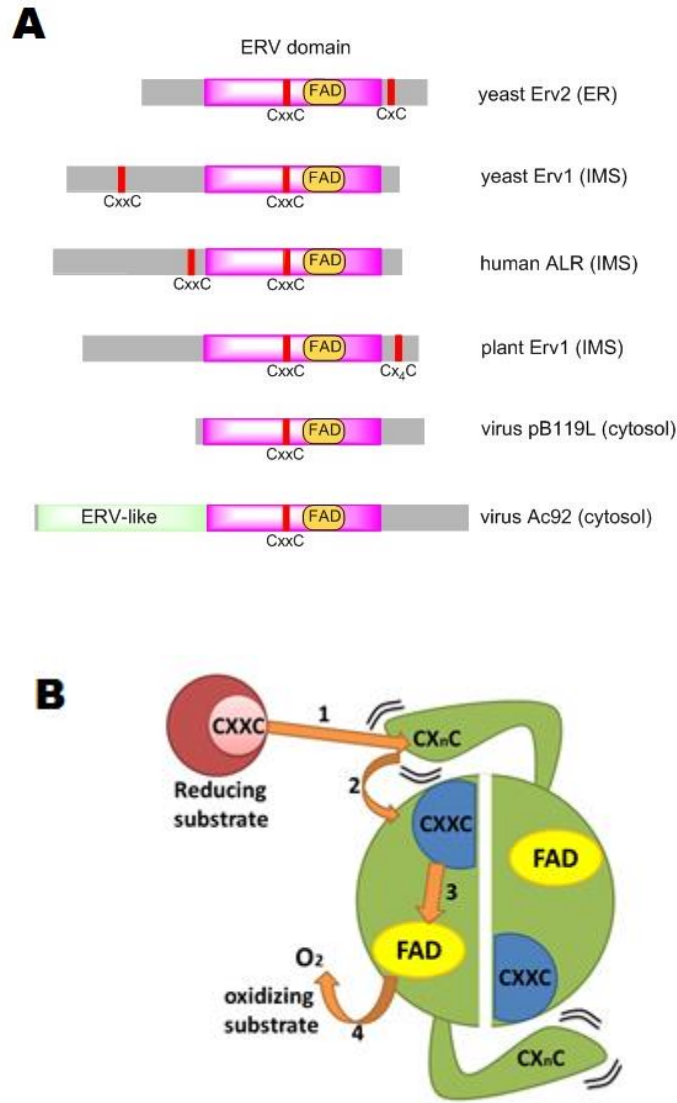


Figure 6: Panel A shows variability in the location of the shuttle disulfide in different organisms, along with where the enzyme is found. The ERV domain is shown in pink and the FAD cofactor is shown in yellow. The proximal CXXC motif is located within the ERV domain and is shown in red. The distal, or shuttle, CXXC motif is located within either the N- or C-terminal extension and is shown in gray. Intracellular locations of the enzymes are in parentheses. Figure adapted from (Thorpe, 2013). Panel B shows proximal CXXC motif and shuttle CX_nC motif communication of a typical single domain ERV/ALR protein. The shuttle disulfide is located on a flexible loop of the protein, at either the N- or C- terminus. Figure adapted from (Vitu et al., 2006).

Erv2p is only found in the Fungi Kingdom and was the first sulfhydryl oxidase to have its crystal structure solved (Figure 7). It revealed the four helix bundle that has become so familiar. How this unique and fascinating secondary structure element came to be in the evolutionary journey remains a mystery yet to be solved (5, 31, 32). The FAD isoalloxazine ring lies in the mouth of the helices while the adenine portion of the cofactor interacts with the shorter 5th helix perpendicular to the axis of the four helix bundle. Though the ERV family is not present in prokaryotes, the four helix bundle is found in many prokaryotic proteins that have redox activity (5, 31-33). Just as in the HRR-ERV pseudo-dimer, helices 1 and 2 are involved in the interface between subunits. ALR (augmenter of liver regeneration), the focus of my project currently, also shares this same interface. This family of enzymes produces quite a bit of superoxide when compared with its QSOX counterpart. About 10% of the total electrons liberated from Erv2p appear as the superoxide. Further, about 30% of the total electrons become the superoxide when the enzyme is forced to adopt a monomeric conformation via residue mutation (5, 34).

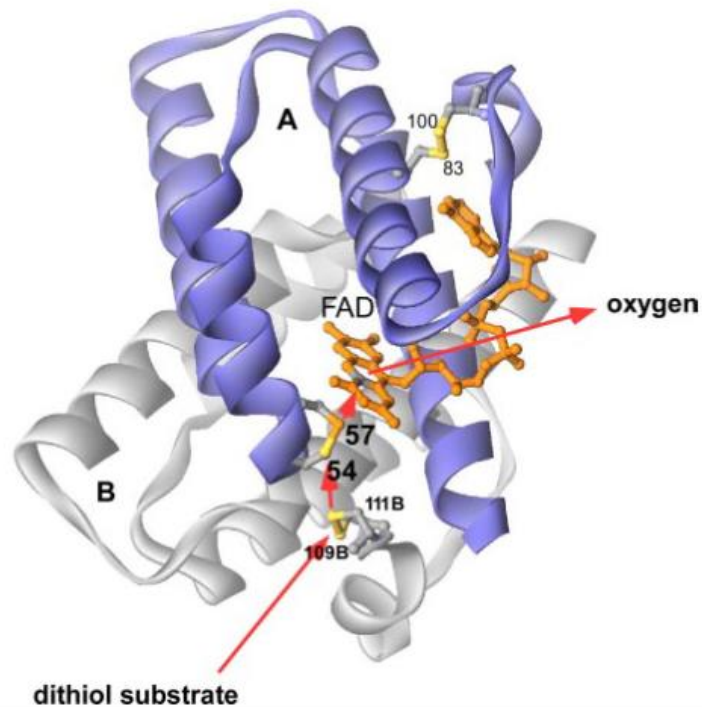


Figure 7: Electron flow during catalysis by Erv2p is represented sequentially by arrows. The two homodimers of the protein are shown in blue and gray. The FAD cofactor is represented in ball and stick form and both the shuttle and proximal CXXC motifs are yellow sticks. In every case studied, the wild-type protein is a homodimer with reducing equivalents from the substrate being passed from the shuttle disulfide of one subunit to the proximal disulfide in the second subunit. Figure taken from (Thorpe and Coppock, 2007) with permission from the publisher.

As mentioned briefly earlier, the intermembrane space of the mitochondria houses a disulfide forming system of its own. The model for this process is represented in Figure 8 (5, 35-38). Mia40 is an integral protein in this disulfide relay system as it interacts with incoming substrates and shuttles the reducing equivalents to the next protein in the relay, Erv1p (yeast)/ALR (mammals), and eventually to oxygen or cytochrome c (30).

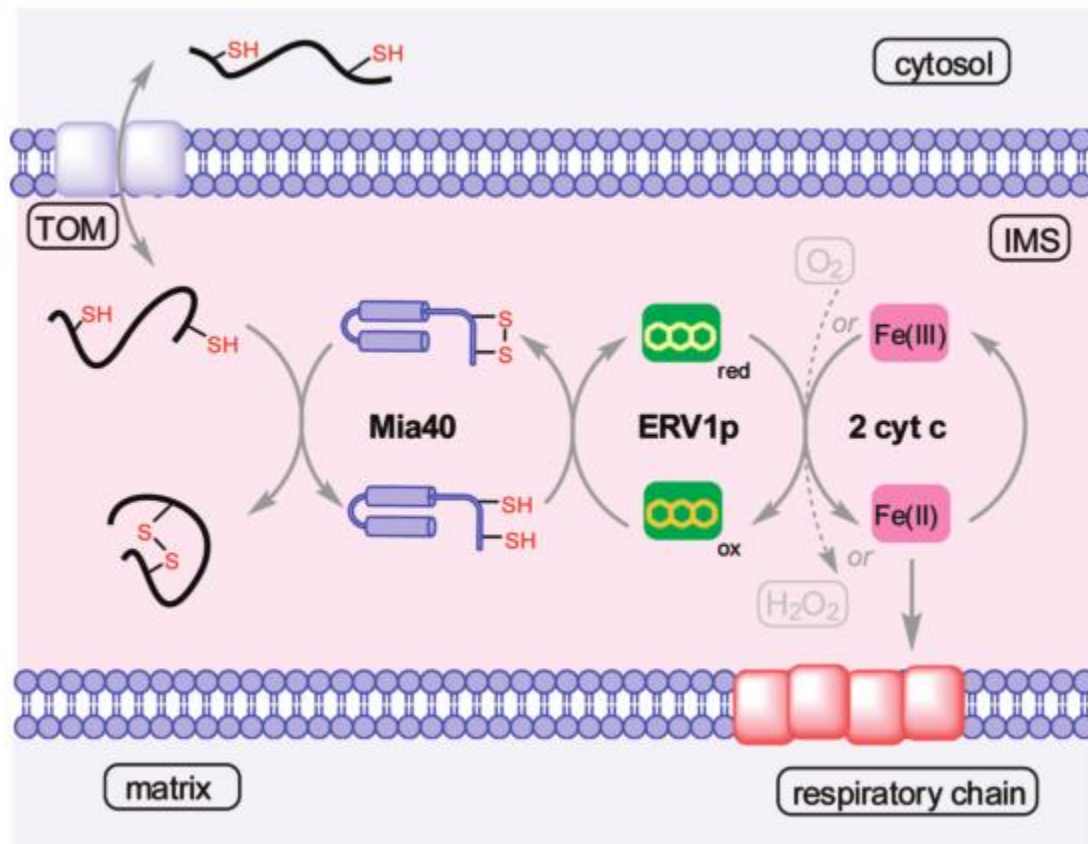


Figure 8: Oxidative folding in the IMS. Either oxygen or cytochrome c reoxidize ALR/Erp1p. Figure taken from (Daithankar et al., 2009) with permission from the publisher.

Mammalian ALR was first discovered in rat blood as a factor that facilitated the regeneration of liver tissue. It was also found to be homologous to the yeast growth factor Erp1p (5, 41). The short form of ALR is responsible for its regenerating functions. This form operates extracellularly and lacks the first 80 amino acids of the N-terminus. This includes the shuttle disulfide. Aside from operating extracellularly, ALR also has intracellular roles (5, 40). The long form of ALR is the form that is responsible for disulfide generation in the IMS of the mitochondria (5, 35-38).

Interestingly, it is also present in the cytosol of the cell where it regulates the growth of liver stem cells (5, 42). Mutating R194 (shown in Figure 9) to H194 in the long form of ALR causes muscle myopathy, cataract, and hearing loss in humans (5, 43) due to a disruption of hydrogen bonds between the ribityl chain of the FAD cofactor and the N and C termini of the protein (5, 40).

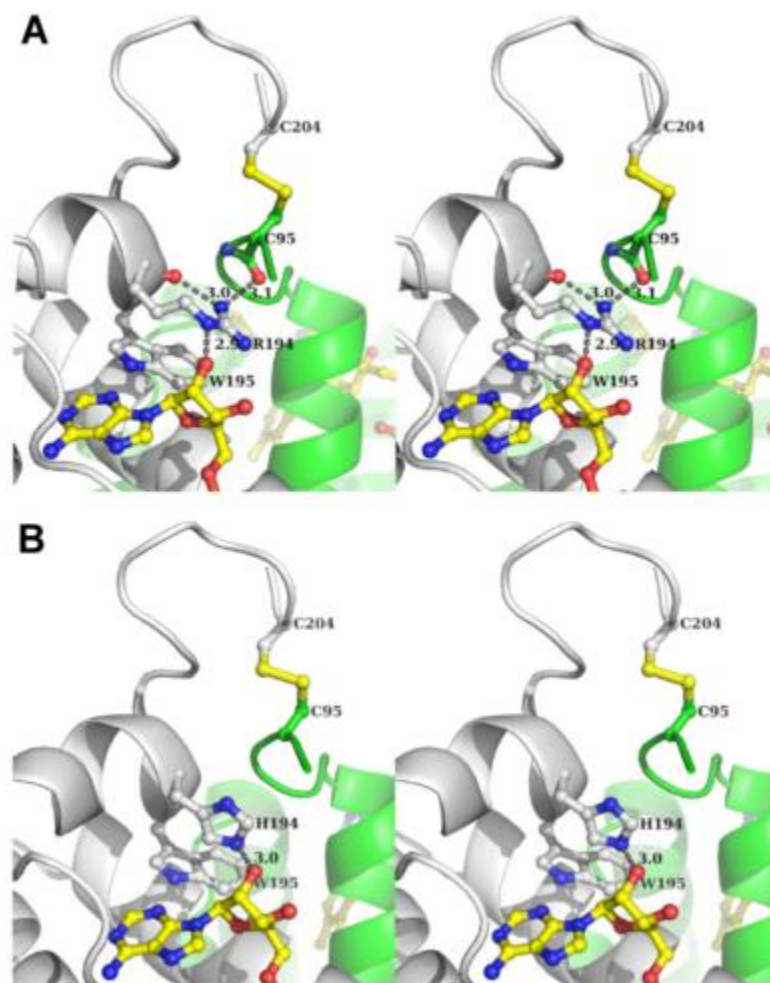


Figure 9: Depiction of R194 H-bond participation in human sfALR and the R194H mutant. Panel A shows that R194 forms H-bonds with the 2' OH of the ribityl moiety of FAD, its own main chain peptide carbonyl, and the main chain carbonyl oxygen contributed by C95 of the other (green) subunit. Panel B shows the interactions of the R194H mutant. Figure taken from (Daithankar et al., 2010) with permission from the publisher.

The short form of ALR shows typical, albeit modest, sulfhydryl oxidase activity with dithiothreitol (5, 14). There were a couple surprises however. The K_m for oxygen was much greater than usual for a sulfhydryl oxidase leading to the discovery

that cytochrome c was a better terminal electron acceptor for both short and long forms of the enzyme (5, 14, 43). In this case, the electrons passed from the substrate could be directly linked to the respiratory chain in the IMS – completely bypassing the production of hydrogen peroxide, as well as the formation of the superoxide ion (5, 35-38).

1.4 Ero1 Family of Sulfhydryl Oxidases

Within the context of a 4-helix bundle, there is an additional family of flavin dependent sulfhydryl oxidases that bind FAD (5). These are the Ero1 family members, and although binding FAD in a similar structural fashion, there is no sequence similarity between the two classes of proteins. Ero1 (shown in Figure 10) was first discovered in *Saccharomyces cerevisiae* and found to exist in two paralogs in mammals (Ero1 α and Ero1 β) (5). As seen in the bottom panel of Figure 2, these enzymes are believed to participate in oxidative folding in the ER by recycling oxidized PDI. Loss of Ero1 function is lethal to both *S. cerevisiae* and *C. elegans*, but mice strains that lack the oxidase show only a minor phenotype (5).

Ero1 proteins are monomers and, as mentioned, bind FAD in a helix-rich domain. The proximal disulfide resides at a turn-helix boundary, much like the ERV family of sulfhydryl oxidases. Both yeast and mammalian enzymes possess a mobile loop that moves the shuttle disulfide in communication with PDI. The mobility of this loop is constrained by regulatory disulfides whose reduction activates both the yeast and mammalian oxidases (5).

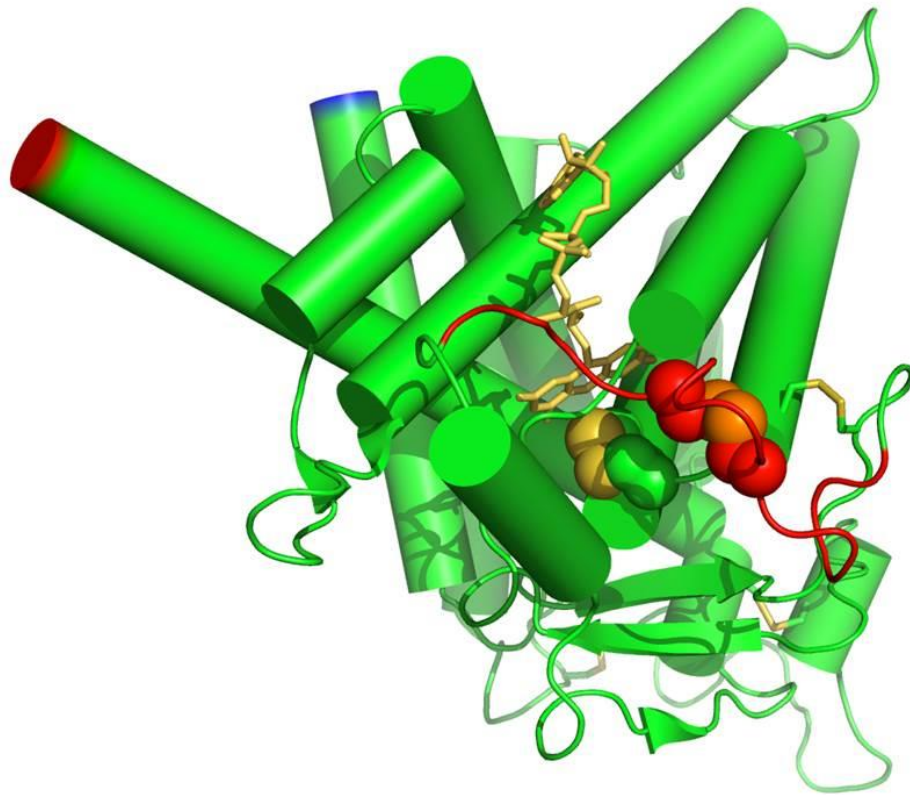


Figure 10: Crystal structure of Ero1 in yeast. The crystal structure of yeast Ero1p. N-terminus is blue. C-terminus is red. The proximal disulfide (yellow spheres) is next to the FAD isoalloxazine ring (yellow ball and stick). The shuttle Cx4C disulfide (orange spheres) is located on a mobile loop (red). Disulfide bonds shown in gold sticks are regulators of oxidase activity. Their reduction initiates the oxidation of reduced PDI by the enzyme. N- and C-termini are depicted in blue and red respectively. Figure adapted from (Thorpe, 2013).

Chapter 2

TRYPANOSOMA

2.1 Physiology

My research project focuses on ALR – specifically the ALR of the *Trypanosoma brucei* parasite (*Tb*ALR, *TbErv1*). Trypanosomes are members of the order Kinetoplastida. There are many different species of trypanosomes that vary in global distribution, vectors used to transmit the disease, and organisms capable of being infected. Trypanosomes are usually grouped into two categories by distribution: 1) African trypanosomes and 2) American trypanosomes (45). Here we focus on the former of the two, since *Trypanosoma brucei* are African trypanosomes.

Trypanosomes are single-celled, flagellated, protists. They have two genomic compartments (46), one in the mitochondria (called the kinetoplast) and the other in the nucleus. The kinetoplast comprises about 10% of the total DNA of the organism. It consists of minicircle and maxicircle DNA and is anchored to the flagellar basal body via protein structures that breach both the outer and inner mitochondrial membranes (46). Trypanosomes only have one mitochondrion. Their chromosomes do not condense during cell division, so the number of chromosomes in the organism remains unknown (45).

The vector for African trypanosomes is the tsetse fly. Both humans and animals (cattle, antelope, horses, camels, donkeys, deer) can contract the disease if bitten by a fly that is a carrier of the trypanosome parasite. Symptoms and duration of the disease differ depending on the species. Humans can contract trypanosomiasis from two trypanosome species: *Trypanosoma brucei gambiense* and *Trypanosoma*

brucei rhodesiense. *Trypanosoma brucei gambiense* is located in West Africa and is a chronic disease, whereas *Trypanosoma brucei rhodesiense* is located in East Africa and is an acute form of trypanosomiasis (45). It is because of the disease's distribution in the poorest areas of the world that the World Health Organization refers to them as a Neglected Tropical Diseases, or NTDs (47).

The tsetse fly becomes infected with bloodstream trypomastigotes when it bites a host that is carrying the parasite. In the midgut of the fly, the trypanosomes transform into procyclic trypomastigotes and multiply via binary fission. The trypomastigotes then leave the midgut of the fly and transform into epimastigotes. It is these epimastigotes that then migrate to the fly's salivary glands, multiple again, transform into metacyclic trypomastigotes, and are ready to infect a host to continue the second half of its life cycle (48). The point up until the host infection takes about three weeks in the fly. When the fly bites a host, the metacyclic trypomastigotes in the fly salivary glands are injected into the host skin tissue where they enter the lymphatic system and the bloodstream. Once in the bloodstream, they transform into bloodstream trypomastigotes. The blood carries the parasites to other organs and eventually to the central nervous system (CNS), all the while multiplying (48).

It is obvious from the parasite's dual life cycle that the location of the parasite at any point in time can be deduced from its morphology. The morphology of the trypanosome depends on its environment. The metabolism of the trypanosome also changes to accommodate its environment. When the parasite resides in the midgut of the fly, it relies on both glycolysis and the citric acid cycle to survive (its mitochondria possesses the typical cytochrome c respiratory chain (45). This makes sense since nutrients are not plentiful. Oxidative phosphorylation can be halted with cyanide in

most organisms because cyanide reacts with cytochrome c oxidase, preventing it from passing reducing equivalents to oxygen to form water. Gut trypanosomes are only partially sensitive to cyanide because they contain an additional cytochrome O, which does not react with cyanide (45).

When the parasite resides in the blood of a mammalian host, it survives purely by means of the glycolytic pathway as its mitochondrion is devoid of TCA cycle enzymes. Since there are so many nutrients available, the parasite doesn't need to squeeze every last drop of energy out of any one nutrient, so to speak, because there is always a surplus of nutrients. Surprisingly, the trypanosome excretes pyruvate, which as one knows will quickly deplete the pool of NAD⁺, as there is no chemical step to re-oxidize NADH (45). This would completely halt the glycolytic pathway. To circumvent this problem, trypanosomes metabolize a product of glycolysis, dihydroxyacetone phosphate, through the glycerophosphate oxidase system. Also interesting to note is the fact that the first nine reactions in the glycolytic pathway are contained in organelles termed the glycosomes (45).

2.2 African Sleeping Sickness

2.2.1 Symptoms

Symptoms experienced by sufferers of *Trypanosoma brucei gambiense* include body aches, weakness, fevers, headaches, swelling of the lymph nodes, and weight loss. The disease is capable of spreading to the body organs and can even cross the Blood Brain Barrier (BBB) to infect the CNS. How far the disease has spread inside the host is often described by stages. Stage 1 refers to the disease before it has spread to the CNS. Stage two refers to the disease once the BBB has been breached and the

parasites reach the CNS. Once the disease spreads to the CNS (within 1 to 2 years), the victim will experience restlessness due to sleep cycle disruption (exhaustion during the day, insomnia at night), personality changes, mental confusion, paralysis, convulsions, coma, and eventually death (48). Interestingly, it is the sleep cycle disturbances experienced by sufferers of the disease that give it the common name of African Sleeping Sickness (47). If left untreated, this chronic form of trypanosomiasis will usually take the victim's life within 3 years (48).

Symptoms experienced by sufferers of *Trypanosoma brucei rhodesiense* are similar to those caused by *Trypanosoma brucei gambiense* but on a much shorter time scale. This species of trypanosome will breach the BBB within weeks and cause death within months (48).

2.2.2 Statistics

In 2012, less than 10,000 cases of African trypanosomiasis were reported. The number of actual cases is estimated to be 30,000, though many cases go unreported and it is difficult to estimate just how many cases of African trypanosomiasis exist. The population at risk of contracting the disease is estimated to be 70 million (47).

2.2.3 Diagnosis and Treatment

Diagnosis of trypanosomiasis is done by microscopy, as the parasite can be easily seen if present in body fluid or tissue. Treatments exist and are dependent on the species of trypanosome and the stage of the disease (48). Though treatments for African trypanosomiasis do exist, adverse side effects of the drugs, drug resistance, and inconvenient administration methods are among their shortcomings. The disease diagnosis, treatment, and any follow-up procedures that need to be done to effectively

rid the patient of the disease and abolish its incidence in the population are expensive (47). In addition, locations that are not properly monitored due to their remoteness or political insecurity do not get reported and do not have access to treatments. Health care facilities are limited, understaffed, and without the state-of-the-art equipment we take for granted (48).

Due to these obstacles, new drugs need to be developed for the disease. The new drugs should be easy to administer by people with no formal training and the treatment duration should be as short as possible. The drug would ideally be able to cure both stages of trypanosomiasis and be easy to transport and store (preferably stable at ambient room temperatures). Of course, the drug should be inexpensive (47).

Pentamidine is a water-soluble aromatic diamidine that has been a treatment for trypanosomiasis for over 70 years. It is effective in treating diseases caused by both *Trypanosoma brucei gambiense* and *Trypanosoma brucei rhodesiense* (less effective) but only if the diseases have not spread to the CNS. Ten intramuscular injections of the drug need to be administered, and even then the trypanosomes may persist in the bloodstream (49).

Berenil, an aromatic diamidine, was originally developed for use in cattle, but has been used in humans. Like Pentamidine, it is effective against early-stage disease caused by *Trypanosoma brucei gambiense* and *Trypanosoma brucei rhodesiense*. Although it is effective and well tolerated by humans, there is no literature regarding toxicity, probably due to the fact that no doctor wants to document using a drug approved for veterinary use on humans (49).

Suramin is a sulfonated naphthylamine that has been successful in treating both African trypanosome species, but it also is only effective before the diseases spread to

the CNS. Once the diseases reach the CNS, an arsenical called Melarsoprol may be given (for both forms of the disease). It is usually administered intravenously three times a day for four days. It is insoluble in water, so it is dissolved in propylene glycol which causes the patient great pain as it destroys the veins after a few doses. Also, since Melarsoprol is indeed an arsenical, it is toxic to patients. Ten percent of patients receiving the treatment died within 48 hours (49).

Difluoromethylornithine (DFMO), also called Eflornithine, is the newest drug for the CNS stage of African trypanosomiasis. It is effective against the disease when given via IV (400 mg/kg) every 6 hours for two weeks. Combining DMFO was drugs like Suramin and Melarsoprol prove to have definite advantages over each drug independently (49).

2.2.4 Trypanosome Variable Surface Glycoproteins and the Host Immune System

Every parasite has one fundamental hurdle to overcome when infecting a host organism and that is the host's immune system. *Trypanosoma* have proved to be unique and interesting organisms thus far, and they quickly become even more fascinating when one considers how the parasite escapes the war zone that is the immune system of the infected species. How do African trypanosomes manage to escape? The answer lies in what are called Variable Surface Antigens or Variable Surface Glycoproteins (VSGs) (45).

Though the African trypanosomes continue to multiply in the host, they do not increase constantly but rather in waves. These waves of population growth are directly proportional to the waves of fever the victim experiences. These waves demonstrate that the victim's immune system almost clears the body of the parasite (wave

minimum) before the parasite population increases again (wave maximum). There must be a change in part of the population that allows it to evade the immune system and produce another generation of parasites (45). This “change” is the coat, or antigen, on the surface of the bloodstream form of the parasite. Trypanosomes taken from different infected hosts showed completely different antigen structures. Even more amazing, trypanosomes taken from different waves of infection in the same host also showed completely different antigen structures. The ability for part of the parasite population to express a different antigen, and hence a different gene, is the reason for trypanosomal survival in the host organism (45).

How does a portion of the trypanosome population change its VSG to elude the host immune system? Each trypanosome only expresses one VSG at a time, so its arsenal of additional VSGs remain silent. When a trypanosome begins expression of a new VSG, the host immune system does not recognize it immediately (45). This gives the population of trypanosomes that are expressing this new VSG time to multiply undetected before the immune system notices its presence. Once the immune response recognizes and begins to address this new population, a different VSG will have already been expressed and the parasite will continue to persist in the host. It is estimated that the trypanosome organism contains 1000-2000 VSG genes, about 10% of the trypanosome genome (45).

How do the trypanosomes have only one active VSG while keeping the other VSGs silent? It is thought that the VSG that is being expressed is actually copied and moved to an active expression site. It is this expression linked copy that is being transcribed and not the copy that permanently resides in the genome. In some cases, an expression linked copy is not created, and the permanent gene is transcribed (45, 50).

Each VSG is approximately 65 kDa and comprised of about 500 amino acids. VSGs comprise 3 protein domains. The N-terminus houses the signal sequence for transport to the plasma membrane. The next 360 amino acids differ greatly from VSG to VSG. The C-terminus is 120 amino acids in length and is very similar from VSG to VSG. The C-terminus contains a hydrophobic tail that includes a signal sequence for attachment to a glycolipid anchor. When the anchor is attached, the signal sequence is cleaved off (45, 51).

The anchor consists of ethanolamine, a glycan structure comprised of mannose moieties, a glucosamine, and a phosphoinositol that is bonded to a 1,2-dimyristoylglycerol buried in the membrane. It's antigenic only *in vitro*. The VSGs are so closely packed on the surface of the trypanosome that the anchor essentially becomes hidden from the host immune system. Trypanosomes are thought to shed their VSGs through the activation of a trypanosome-specific phospholipase C that is thought to be present on the inner face of the plasma membrane. The enzyme cleaves the phosphodiester bond linking the VSG to the membrane surface, releasing the VSG (45, 51).

Each domain contains a conserved pattern of cysteines, with three different types of patterns in the variable region and four in the C-terminus. This conservation of cysteine residues in the variable region is the only homology within that region of the VSG (52). The variable region of the monomeric protein is comprised of 2 alpha helices, forming a coiled coil. Since VSGs are homodimeric, these N-terminal domains form 4 helix bundles. Despite variation in this region, the tertiary structure of VSGs remain conserved, which is important for their close packing on the surface coat (about 5 million VSGs per cell) (52, 53).

Though the C-terminus is similar from VSG to VSG, it is physically hidden from the immune system because it is bound to the plasma membrane. The glycolipid anchor, shared by all VSGs, is thought to only be antigenic when shed from the membrane due to the close packing of VSGs on the surface of the trypanosome (45, 51).

2.2.5 Sulfhydryl Oxidases Present in Trypanosomes

There are three FAD dependent sulfhydryl oxidases in African trypanosomes. One is homologous to yeast and metazoan Ero1, resides in the ER, and is thought to participate in oxidative protein folding (see Figure 2, bottom panel). The second is a QSOX protein (21). Interestingly, in *Tb*QSOX, the distal disulfide is part of a CGAC motif preceded by a glycine whereas QSOXs from birds and mammals employ a CGHC motif preceded by tryptophan. Along with these 6 conserved cysteines, *Tb*QSOX has an additional 8 cysteines probably participating in disulfide bridges in the monomer. Of these additional 8 cysteines, half are non-conserved among QSOXs in other eukaryotic species (21).

*Tb*QSOX shares a similar optimal pH (approximately 7) with metazoan QSOX. The catalytic efficiencies of *Tb*QSOX in rRNase oxidation are 3-6-fold lower when compared to the avian, milk, and human enzymes. *Tb*QSOX also shows a 2-fold lower catalytic efficiency when compared to avian enzyme for the oxidation of RfBP. Trypanothione shows a catalytic efficiency 10 fold lower than both rRNase and RfBP (21).

The third protein, *Tb*ALR, is the focus of my research project. From a multiple sequence alignment (Figure 11) (54), one can draw a schematic of the proteins and denote the locations of the cysteine residues (Figure 12).

```

sp|P55789|ALR_HUMAN          -----MAAPGERGRFHGGNLFLLPGGAR--SEMMDDLATDARGRGAGRR 42
sp|P27882|ERV1_YEAST        MKAIDKMTDNPPEGLSGRKIIYDEDGKP--CRSCNTLLDFQYVTGKISN 48
gi|71744716|ref|XP_826988.1| -----MSKQEPLOKIPGECPTPRELGKAGWIIHLSAAAVFPYNPTPTQQ 44
                               *:      : *      *      .      .

sp|P55789|ALR_HUMAN          DAAASASTPAQAPTSDSPVAEDASRRRPCRACVDFKTMRTQQKRDIKFR 92
sp|P27882|ERV1_YEAST        GLKNLSSNGKLAGTG--ALTGEASELMPG-----SRTYR 80
gi|71744716|ref|XP_826988.1| EAFRNFLHGWSHAYACSHCAYHMRRYFHQNPVVDKLLALNRYLCEFHNA 94
                               .      :      .      .

sp|P55789|ALR_HUMAN          EDCPPDREELGRHSWAVLHTLAAYYPDLPTPEQQQDMAQFIHLFSKFYPC 142
sp|P27882|ERV1_YEAST        KVDPPDVEQLGRSSWILLHSVAASYPAQPTDQQKGEMKQFLNIFSHIYPC 130
gi|71744716|ref|XP_826988.1| VNERVGNKIYDCPMNVLRRWHPFPDMEDQPTIEEQVKSLELKEKNETP 144
                               . : . . : * : . : * : : : : .

sp|P55789|ALR_HUMAN          EECAEDLRKRLCRNHDP-----TRTRACFTQWLCHLHN 175
sp|P27882|ERV1_YEAST        NWCAKDFEKYIRENAPQ-----VESREELGRWCEAHN 163
gi|71744716|ref|XP_826988.1| QGVSDRWRRQQSSASPDNGVGRWSVGDARWTDITSESRRTINVEISAGWG 194
                               : :. .: * : . : * : .

sp|P55789|ALR_HUMAN          EVNRKLGKPD-----FDCSKVDERWRDCGWKDGSCD----- 205
sp|P27882|ERV1_YEAST        KVNKCLRKPK-----FDCNFWEKRWDGCWDE----- 189
gi|71744716|ref|XP_826988.1| TAGEKMKQRNSAGDGVSDAGASEKKWWR-WGNSTSSSTTATATPSAAEP 243
                               ...* : . *.. : : * * :

sp|P55789|ALR_HUMAN          -----
sp|P27882|ERV1_YEAST        -----
gi|71744716|ref|XP_826988.1| AEDVEASVTSILSKLRACMVYCPDDKKSSA 273

```

Figure 11: ClustalW2 multiple sequence alignment of human lfALR, yeast Erv1, and TbALR. Cysteine residues are highlighted in pink.



Figure 12: Domain representation of yeast Erv1, human lfALR, and TbALR. FAD is represented by yellow hexagons. Cysteines are represented by yellow bars. The ERV/ALR domain is green, while the rest of the protein is blue.

The crystal structure of Erv1 (Figure 13) gave insight into the mechanics of the disulfide relay system in yeast. After a reduced substrate is oxidized and released, the

hydrophobic cleft of Mia40 becomes exposed. The amphipathic helix at the shuttle domain of Erv1 interacts with the hydrophobic cleft of Mia, facilitating the electron transfer and propagating the disulfide relay. Electron transfer from Mia40 to Erv1 requires mechanisms to circumvent the unfavorable redox gradient (30).

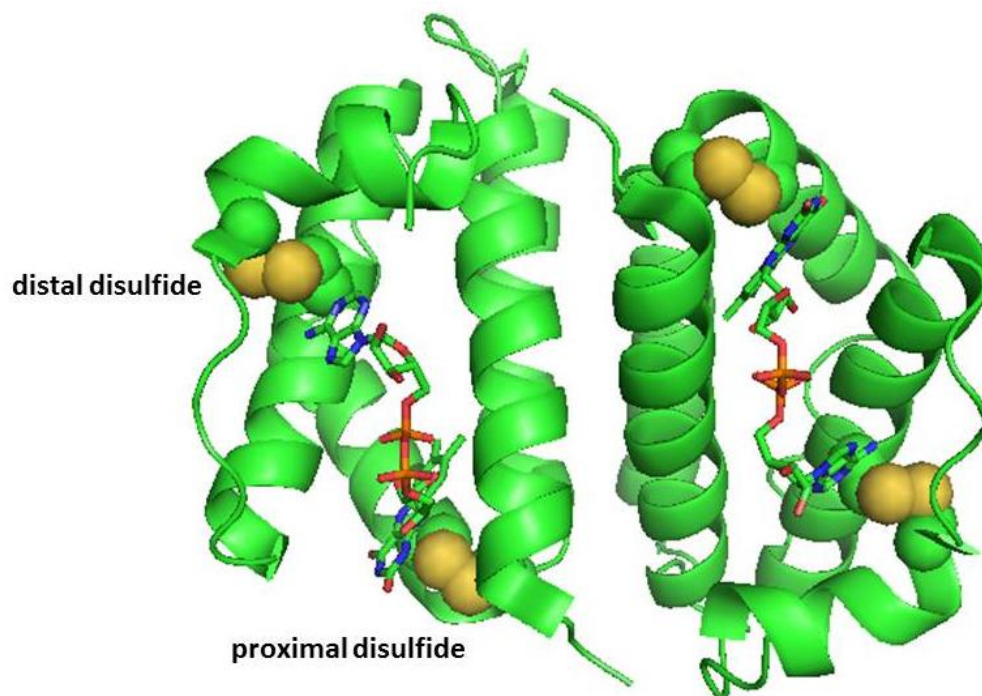


Figure 13: Crystal structure of yeast Erv1 shows the redox-active proximal (C130–C133) and distal (C30–C33) disulfides and the structural disulfide (C171–C188) depicted as yellow spheres. The FAD is depicted in ball and stick form.

Chapter 3

OXIDATIVE FOLDING AND THE DISULFIDE RELAY SYSTEM IN THE INTERMEMBRANE SPACE (IMS) OF MITOCHONDRIA IN MOST EUKARYOTES

3.1 Mitochondria

The mitochondria are comprised of two membranes, the outer and inner membrane, each of which surround a hydrophilic compartment (the intermembrane space and the matrix, respectively). The matrix houses hundreds of proteins that participate in various cellular functions such as aerobic oxidative metabolism, respiration, and iron-sulfur cluster maturation (7). Most of these proteins are translated on cytosolic ribosomes and must be imported into the matrix via the translocase of the outer membrane (TOM complex) and translocase of the inner membrane (TIM complex). Import is signaled by aminoterminal matrix targeting signals, or MTSs. These MTSs are removed via protease by the matrix processing peptidase once the protein is transported into the mitochondria (7).

3.2 The Intermembrane Space and the Mitochondrial Intermembrane Space Assembly Pathway

The IMS houses a lesser amount of proteins than the matrix, but these proteins still carry out important functions in the cell including transport of biological molecules in between the membranes of the mitochondria and cell: mitochondria communication. The IMS also participates in regulating apoptosis. All proteins found in the IMS are synthesized in the cytosol. Unlike proteins that are targeted to the matrix, proteins targeted to the IMS do not have MTSs (7). The IMS imported proteins are dependent upon a disulfide relay system known as the mitochondrial

intermembrane space assembly (MIA) pathway (55). Many of the proteins imported use internal sequences to initiate their import (7).

Cysteine residues play a significant role in these sequences. These sequences are referred to as MISSs, or mitochondria IMS-sorting signals. Cysteine residues in the MISSs are recognized by an oxidoreductase in the MIA pathway, Mia40. Mia40 is kept in an oxidized state by the sulfhydryl oxidase Erv1, a second and critical protein in the pathway (7).

3.3 Substrates of the Intermembrane Space Assembly Pathway

What types of proteins are imported into the IMS? What are Mia40's substrates? Substrates of the IMS disulfide relay system can be divided into two categories: 1.) Twin CX₃C proteins and 2.) Twin CX₉C proteins (7).

The twin CX₃C proteins facilitate the transport of hydrophobic proteins across the IMS through the formation of heteromultimeric complexes. Members of this group include the Tim proteins. They have a helix-loop-helix fold, with each helix containing two cysteine residues in a parallel disulfide bridge separated by 3 amino acids, hence the term "CX₃C protein." The cysteines are critical for import into the IMS, correct folding, and complex formation. Mohr Tranebjaerg syndrome is caused by a mutation in the human homolog of Tim8, DDP1 (7). Twin CX₉C proteins also share the same helix-loop-helix fold, except that the pairs of parallel disulfide bridges are nine residues apart and not three. The most well-known member of this group is Cox17. Other CX₉C proteins are required for the respiratory chain complex formation, but their exact function remains cryptic (7).

Additional proteins that depend on the disulfide relay system for import into the mitochondria include Mia40 and Erv1 themselves. Mia40 contains the typical

CX₉C motif, but Erv1 shares neither helix-loop-helix structure. Other proteins that do not share the typical structure of a Mia40 substrate exist, but are few and far between (7).

How are substrates imported to the mitochondria? After being translated by cytosolic ribosomes, the protein substrate must pass the outer membrane first. Substrates must be both unfolded and reduced. Mia40's redox active CPC motif is responsible for covalent interaction with substrates. The CPC motif is followed by the familiar helix-loop-helix structure (7). As one might expect, the inside of the two helices is hydrophobic while the outside of the helices is hydrophilic. It is this hydrophobic area that is thought to be the location that interacts with the helix-loop-helix regions of substrate proteins. Mutating any residue within the hydrophobic region of Mia40 with a charged residue diminishes its activity (7).

The sequences LXXXCF and aromatic-XX-hydrophobic-hydrophobic-XXC were recently discovered to be the MISSs for CX₃C and CX₉C substrates, respectively. The cysteine in these MISSs is proximal to the CPC motif of Mia40 and will attack via thiolate. Aside from this, the full details of the mechanism remain unknown (7).

After substrate oxidation, reduced Mia40 is subsequently oxidized by Erv1. The second cysteine of Mia40 is thought to form a mixed disulfide with the second cysteine of the distal disulfide in Erv1, as these are the only cysteines required for the electron transfer to occur. Erv1 can then pass its electrons on to oxygen or cytochrome c (7). When cytochrome c is the terminal electron acceptor, it accelerates the oxidation of Mia40 both *in vivo* and *in vitro*. Cytochrome c can then be oxidized by cytochrome c oxidase of the respiratory chain, producing water instead of hydrogen peroxide.

Which pathway predominates is unknown, however mutations leading to the inactivity of cytochrome c does indeed hinder Mia40's oxidation (7). A schematic showing the IMS disulfide relay system was shown in Figure 8.

Chapter 4

OXIDATIVE FOLDING AND THE DISULFIDE RELAY SYSTEM IN THE INTERMEMBRANE SPACE (IMS) OF THE MITOCHONDRION IN TRYPANOSOMES

There are some unicellular eukaryotes that lack the substrates of the MIA pathway, as well as a Mia40 homologue. Fascinatingly, there are some unicellular eukaryotes that contain the substrates for the MIA pathway but lack a Mia40 homologue. *Trypanosoma* fall into this fascinating category (55).

It is hypothesized that trypanosomes import proteins into the IMS using a pathway more ancestral than the MIA pathway, and as such is representative of the import pathway that would have been used by early eukaryotes. Perhaps the oxidation of substrate proteins was accomplished through an interaction with Erv1. Erv1 is indeed a sulfhydryl oxidase and in the absence of Mia40, this seems quite plausible. After all, other sulfhydryl oxidases are present in the cell and function without Mia40 (55).

RNA interference (RNAi) against *TbErv1* resulted in the same mitochondrial swelling as observed by epifluorescence microscopy following RNAi against trypanosomal Tim proteins. This suggests a direct role for *TbErv1* in mitochondrial IMS protein import. Though a direct role is suggested, *TbErv1* was not able to catalyze the oxidative folding of a small Tim *in vitro*, therefore it is still plausible that *TbErv1* performs in unison with a Mia40 homolog. Interestingly enough, *Trichomonas*, another protozoan parasite, lacks both Erv1 and Mia40. *Trichomonas* also possess Tim proteins that lack disulfide bonds (56).

The physiological electron acceptor for Erv1 in *S. cerevisiae* and mammals is cytochrome c. The electron acceptor for Erv1 in trypanosomes is less clear since, as discussed earlier, only the tsetse fly form of the African trypanosome is capable of utilizing oxidative phosphorylation for energy. Erv1 can reduce either cytochrome c or O₂ as alternate substrates. Cytochrome c was reduced 58% slower under aerobic conditions when O₂ was also a substrate than when cytochrome c was used as the substrate alone under aerobic conditions (56). *TbErv1*'s use of both cytochrome c and O₂ as substrates is consistent with both the physiology and the morphology of trypanosomes. In the bloodstream form of the parasite, cytochrome c is not available. O₂ remains the only logical choice for an electron acceptor. In the tsetse fly form of the parasite, cytochrome c becomes a viable electron acceptor (45).

It is also apparent that though Erv1 has the ability to reduce both substrates, it does have a preference for O₂. One reason for this is the conservation of residues predicted to compromise a hydrophobic channel from Erv1's surface to its cofactor – specifically to the N5 nitrogen of the FAD isoalloxazine ring. Mutation of these conserved residues (His-66 and Tyr-70) resulted in unstable but active protein (56).

As one would expect, and as observed with *S. cerevisiae* and mammalian ALR, mutation of the cysteines proximal to the FAD cofactor inactivates *TbErv1* for the oxidation of both DTT and the phosphine, TCEP, and the reduction of both cytochrome c and O₂. As one would also expect, mutation of the distal disulfides of *TbErv1* did not render the enzyme inactive for the small substrate, DTT. Surprisingly, however, and in stark contrast to sulfhydryl oxidases exhibiting a similar catalytic FAD core and dimer formation, *TbErv1* was still able to oxidize the larger substrate, TCEP, with its distal disulfides mutated. This points to the conclusion that

trypanosomal Erv has an active site that adopts a more open conformation – a conformation which the substrate can more easily access (56).

Other differences beside the lack of Mia40 in the MIA pathway exist in trypanosomes. The Tim17-Tim22-Tim23 family of proteins is conserved in eukaryotic organisms and required for proteins to insert into the inner mitochondrial membrane (TIM23 complex) and transport into the matrix (TIM22 and TIM23 complexes) (46). This family of proteins participates in two separate membrane complexes. In *Trypanosoma brucei*, there is only one member of the Tim17-Tim22-Tim23 family of proteins encoded in the genome. This suggests a translocase that can perform the functions of both complexes (46). A further example of multiple protein functions in higher eukaryotes seemingly fused into one protein in trypanosomes, include the Tim8 and Tim13 proteins. Trypanosomes express one protein that has sequence features of both of these human proteins (46).

In addition to the TIM proteins mentioned above, trypanosomes (and other members of their Euglenozoa phylum) possess cytochrome (c and c1) with covalently attached heme through a single cysteine residue in an AXXCH motif (X is never cysteine). This is markedly different from all other eukaryotes that utilize a dual cysteine attachment via a CXXCH motif (X is never cysteine) (55).

Trypanosomes lack genes for glutathione reductase, thioredoxin reductase, and catalase and selenocysteine-containing glutathione peroxidases. Most eukaryotes utilize the glutathione/glutathione reductase and thioredoxin/thioredoxin reductase redox couples to regulate the redox state of the cell interior. Trypanosomes utilize a trypanothione/trypanothione reductase pair to buffer intracellular disturbances in redox state (57). Trypanosomes possess a small arsenal of low molecular weight

thiols: trypanothione (T(SH)₂), glutathione (GSH), mono-glutathionylspermidine (Gsp), and ovothiol A (OvSH). Using the model organism, *Crithidia fasciculata*, it has been shown that growing cells experience an increase in trypanothione production, while cells in the stationary phase experience a decrease in trypanothione concentration but an increase in mono-glutathionylspermidine. This phenomenon is thought to free the polyamine, spermidine, which is essential for cell proliferation (57).

Trypanothione reductase (TR), not surprisingly, is an FAD dependent oxidoreductase and is quite similar structurally and chemically to glutathione reductase and thioredoxin reductase (both of which trypanosomes lack), with glutathione reductase (GR) being its closest relative (57). All of these enzymes are homodimers with each monomer having a molecular weight of around 50 kDa. The most significant difference between TR and GR is the substrate binding site. TR has a wider and more negatively charged site that will better interact closely with its glutathionylspermidine substrates. The most plentiful dithiol protein in African trypanosomes are the tryparedoxins (TXNs), which employ a WCPPCR motif in the active site. Though not similar to thioredoxin proteins in sequence, structurally both Trxs and TXNs have the same core structure (57).

To describe the “whole picture” view of the thiol based redox metabolism in African trypanosomes: Two glutathione molecules and a single spermidine molecule form trypanothione in a reaction catalyzed by trypanothione synthetase (TryS). GSH is produced from glutamate, cysteine, and glycine in a dual step process by γ -glutamylcysteine synthetase and glutathione synthetase. Spermidine is produced from ornithine by ornithine decarboxylase (ODC) (57). ODC produces putrescine, which is

linked with an aminopropyl group. This reaction involves the enzyme spermidine synthase. In the cytosol, T(SH)₂ reduces proteins like thioredoxin (Trx), trypanredoxin, and glutathione disulfide as well as dehydroascorbate (57). The then oxidized trypanothione is reduced by trypanothione reductase, which is dependent upon reducing equivalents from NADPH. T(SH)₂ can be bound to metal-containing drugs. 2-Cys-peroxiredoxins and enzymes like glutathione-peroxidase convert hydroperoxides into alcohols (57). TXN also shuttles electrons to ribonucleotide reductase, which makes the deoxyribonucleotides for DNA synthesis. In the mitochondrion, there exists an isoform of TXN that transfers electrons to peroxidases, the universal minicircle sequence binding protein (UMSBP), and a monothiol glutaredoxin. USBBP is involved in the replication initiation kinetoplast (K)-DNA. 1-C-Grx1, which is thought to participate in iron metabolism and/or in the biogenesis of Fe-S clusters. Since TR and TryS are not detectable in the kinetoplast, perhaps trypanosomes have a mechanism to shuttle these enzymes between the cytosol and the mitochondria (57).

Chapter 5

PREVIOUS WORK WITH QUIESCIN SULFHYDRYL OXIDASE 2 AND TRYPANOSOMA BRUCEI AUGMENTER OF LIVER REGENERATION

5.1 Quiescin Sulfhydryl Oxidase 2

My original project was to express, purify, and characterize a member of the QSOX family previously mentioned, QSOX 2. Due to an impasse with the project, I moved on to working with augmenter of liver regeneration from *Trypanosoma brucei* (TbALR). My previous work with QSOX 2 will be only briefly mentioned here.

The project was initiated by Mr. Benjamin Israel. Trying different combinations of cell lines and growth/expression temperatures, it was decided that purifying under denaturing and reducing conditions from BL21*DE3 cells would provide the most amount of protein. Even still, some of the protein remained insoluble. Several different attempts to purify and refold the protein were made with little success. The protein would not bind its FAD cofactor. I spent almost one full year trying to obtain active protein. It was decided that it would better to move on to characterizing a new protein – ALR from *Trypanosoma brucei*.

5.2 Trypanosomal Augmenter of Liver Regeneration

This project was originally initiated by an undergraduate at the time, Ms. Amy Styer, in an effort to probe the MIA pathway in trypanosomes. The ALR cDNA from *Trypanosoma brucei* was designed by Dr. Vamsi Kodali, synthesized using codons optimized for expression in *E. coli*, and cloned into a pET28 vector with a His-tag at

the N-terminus. BL21*DE3, Origami 2(DE3), and Shuffle T7-Express cells were all used to express the protein (transformations performed by Ms. Amy Styer), and in all cases the protein was predominantly found in the insoluble fraction, though some protein was still present in the soluble fraction. *Tb*ALR is a 32.6 kDa protein comprised of 293 amino acids. This includes the 6X His-Tag at the N-terminus along with fourteen other non-native amino acids in the sequence. It has seven native cysteines, one of which is mutated to a serine at the fourteenth position (to be described). The full sequence of the construct used is as follows:

MGSSHHHHHSSGLVPRGSHMSKQEPLQKIPGECPTPR
ELGKAGWIILHSA AAVFPYNPTPTQQEA FRNFLHGWSH
AYACSHCAYHMRRYFHQNPPVVTDKLLALNRYLCEFHN
AVNERVGNKIYDCDPMNVLRRWHPTFPDMEDQPTIEEQ
VKSLELKEKNETPQGVSDRWRQQNSSASPDGNVGRWS
VGDARWTDTTSESRRTNVGEISAGWGTAGEKMKQRNS
AGDGVSDAGASEKKWWRWGNSTSSSTTATIATPSAAEP
AEDVEASVTSILSKLRACMVYCPDDKKSSA

Ms. Styer had difficulties working with *Tb*ALR from the very beginning. The protein expressed well, but purification procedures proved to be replete with obstacles. Protein purity following Ni-NTA chromatography was inadequate. The SDS-PAGE gel of soluble (expression at 15 °C) wild-type (WT) *Tb*ALR shows the presence of lower molecular weight contaminants (Figure 14). The more prominent of these was sent to a former lab member, Dr. Shawn A. Gannon, to be analyzed using mass

spectroscopy. It was shown to be a protein fragment of *TbALR*. Subsequent data by Dr. Vidyadhar Daithankar showed that the intensity of the band on an SDS-PAGE gel increased with time. This led to the conclusion that the fragment is a product of proteolysis at the C-terminus, since it co-purifies with N-terminal His-tagged *TbALR*.

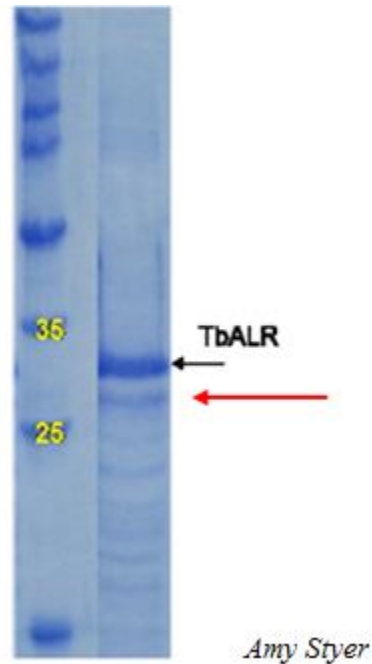


Figure 14: SDS-PAGE gel of soluble WT *TbALR* after Ni-NTA chromatography. Lane 1 is the protein marker (molecular weights in yellow; kDa). The red arrow indicates the *TbALR* proteolysis contaminant.

TbALR also irreversibly aggregated on Ni-NTA resin, as well as the cobalt-based TalonTM resin. *TbALR* has 7 cysteines, one thought to be unpaired at the N-terminus. This unpaired cysteine, C14, was mutated to a serine using site directed mutagenesis in an effort to prevent aggregation. This mutant, denoted *TbALR*' , did not affect enzymatic activity and so was used throughout the rest of Ms. Styer's

experiments, as well as my own. Moreover, *TbALR* also aggregated irreversibly while concentrating on the Centricon® membranes. The C14S mutant did not prevent aggregation in any of these protocols.

Purification from inclusion bodies was also attempted by Ms. Styer (expression at 37 °C vs. 15 °C). *TbALR* inclusion bodies must first be denatured, reduced, and then refolded to the native state. Most procedures employ “flash dilution,” where protein is added to an excess of buffer. The idea behind this is that upon dilution the protein concentration will be too small to facilitate aggregation; however, *TbALR* precipitated using this procedure. The opposite of the “flash method” – slowly adding buffer to the protein – proved successful for refolding the protein. As seen in the SDS PAGE in Figure 15, purification from inclusion bodies resulted in less contaminants but not ideal purity. As seen on the SDS-PAGE gel, the proteolytic fragment is still present.

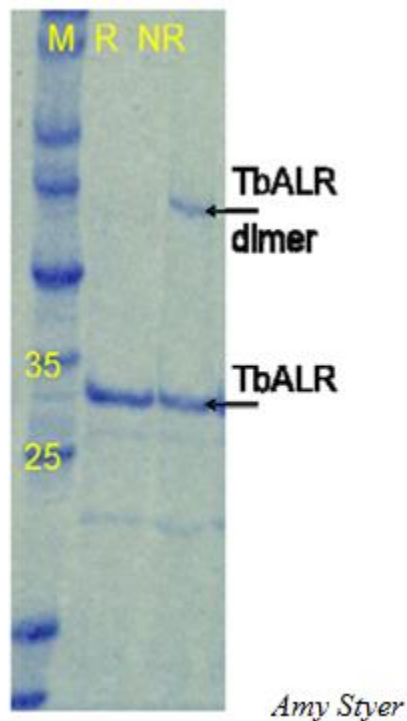


Figure 15: SDS-PAGE gel of TbALR' after inclusion body purification and the novel refolding method. Lane 1 is the protein marker (molecular weights in yellow; kDa). Lanes 2 and 3 are under reducing and non-reducing conditions, respectively. The red arrow indicates the TbALR proteolysis contaminant.

Optimal concentration, dialysis and purification methods for *TbALR'* remain unresolved as all conditions Ms. Styer tested still resulted in some precipitation of the protein.

Dr. Daithankar continued the work of Ms. Styer in the Thorpe lab (with the *TbALR* C14S mutant). He subcloned the protein into pGEX4T3 and pTricHisA, transforming each into the three strains of *E. coli* mentioned previously. pTricHisA vectors showed no expression. pGEX4T3 showed all protein in the insoluble fraction with expression at 15 °C, as well as 37 °C. The eukaryotic expression system, *Pichia*

pastoris was also used with pPicZαA and pPicZB vectors, but minimal expression was obtained. Inclusion body purification was decided as the best way to obtain the protein. This process was carried out with *E. coli* BL21*DE3 cells.

Dr. Daithankar modified Ms. Styer's modifications slightly and lysed the cells under denaturing and reducing conditions. The protein was then bound to an Ni-NTA column, eluted, and refolded. Figure 16 shows an SDS-PAGE gel of *TbALR'* following this protocol. As can be seen from the SDS-PAGE gel, the proteolysis fragment is still present.

Dr. Daithankar also performed preliminary assays on *TbALR'* protein using the model substrate, DTT. The extinction coefficient was determined to be $11.3 \text{ mM}^{-1} \text{ cm}^{-1}$ at 456 nm. *TbALR'* shows maximal activity around pH 9 and modest sulfhydryl oxidase activity with k_{cat} and K_{m} values of 145/min and 16 mM, respectively (Figure 17). The K_{m} for DTT is higher when compared to sfALR (2 mM) and lfALR (3 mM). $k_{\text{cat}}/K_{\text{m}}$ values at pH 7.5 for *TbALR'* are comparable at $545 \text{ M}^{-1} \text{ s}^{-1}$.

Though active protein was obtained with fewer complications than arose with Ms. Styer's procedure, the issue of sub-optimal purity still remained. A higher protein purity is desirable for future assays and experiments – one focus of which is solving the crystal structure. This is where my project began.

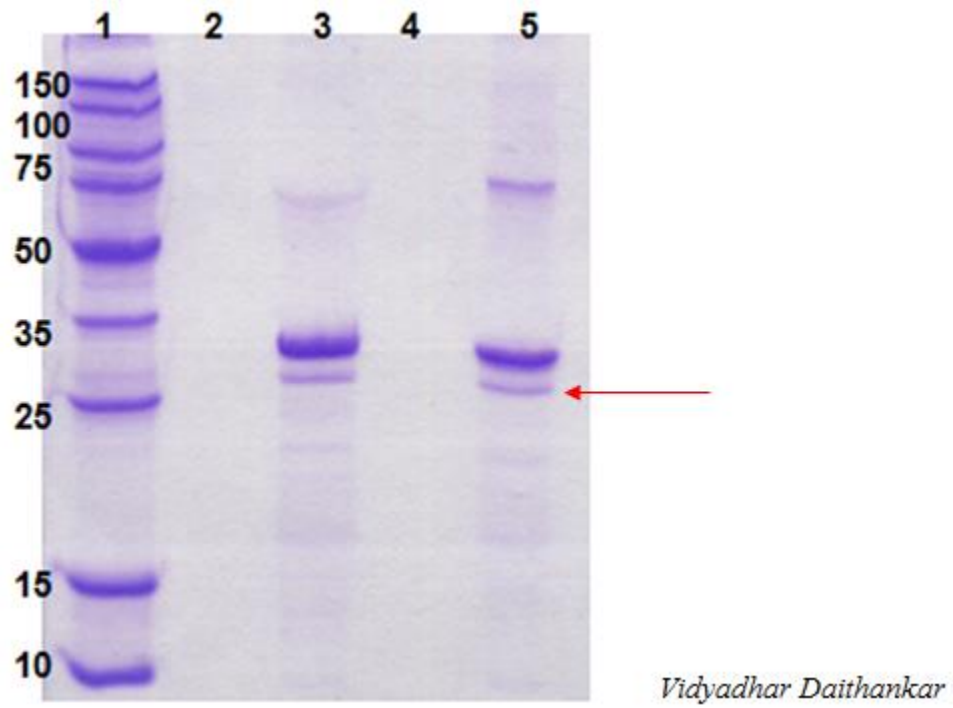
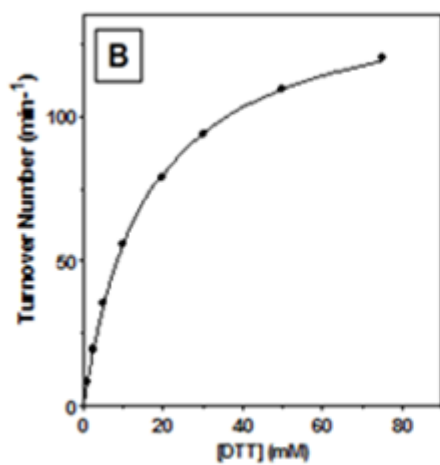
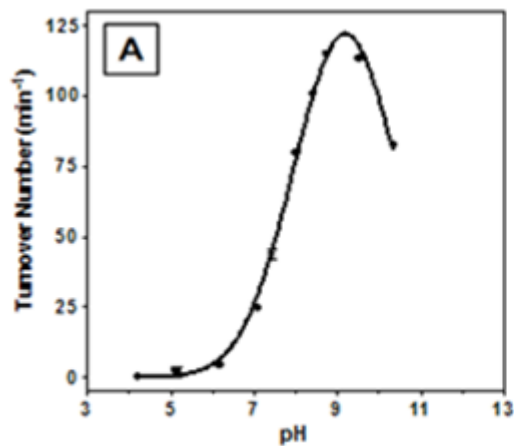


Figure 16: SDS-PAGE gel of TbALR' following lysis under denaturing and reducing conditions. Lane 1 is the protein marker (molecular weights on the left; kDa) Lane 3 is under reducing conditions. Lane 5 is under non-reducing conditions. The red arrow indicates the TbALR' proteolysis contaminant.



Vidyadhar Daithankar

Figure 17: Catalytic parameters for TbALR' (‘ indicates C14S mutant). Panel A. pH profile of TbALR' with 10 mM DTT shows an optimal pH around 9.0. Panel B. Michaelis-Menten parameters for TbALR' using DTT as a substrate in oxygen electrode assay.

Chapter 6

CURRENT WORK WITH TRYPANOSOMA BRUCEI AUGMENTER OF LIVER REGENERATION

6.1 Protein Purity Improvement Using Inclusion Body Purification

I began inclusion body purification in an effort to obtain purer protein. Expression was carried out in BL21*DE3 cells. One millimolar IPTG was added when the cells achieved an OD₆₀₀ of 0.8. Expression continued for 6 hours. Cells were harvested, resuspended using a buffer of 50 mM Tris containing 500 mM NaCl, 1 mM PMSF, and 0.1 mg/mL lysozyme, pH 7.5, and lysed via French press (2x). The lysed cells were then sonicated (3x, 10s). The cell pellet was resolubilized using a buffer of 50 mM Tris containing 500 mM NaCl, 5M Guanidine Hydrochloride, and 15 mM β-Mercaptoethanol, pH 7.5. The solubilized protein was then renatured using a buffer of 50 mM Tris and 500 mM NaCl, pH 7.5.

As can be seen from the following SDS-PAGE gels, a significant amount of protein is expressed (Figure 18) and it is already relatively pure after cell lysis (Figure 19). Upon denaturing and reducing the protein, all of the protein is soluble and ready to be refolded through slow addition of renaturing buffer (7x the protein volume) (Figure 19). Data obtained from a preliminary oxygen electrode assay (5 mM DTT and 20 mM DTT; data not shown) compared with the data shown Figure 17, provided confidence that the protein obtained using this method of inclusion body purification did result in active protein.

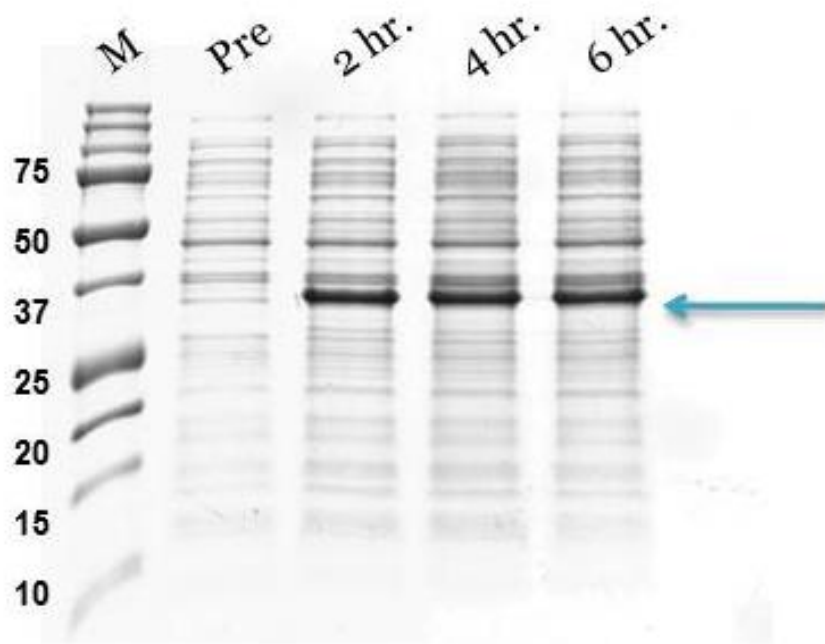


Figure 18: Expression gel of TbALR⁷. IPTG induction, BL21*DE3 cells, 37 °C. Lane 1 (M) is the marker. Molecular weights of the marker are in kDa. Lane 2 (Pre) is the pre-induced sample. Lanes 4-6 are hours 2-6 post induction. TbALR⁷ is indicated by a blue arrow.

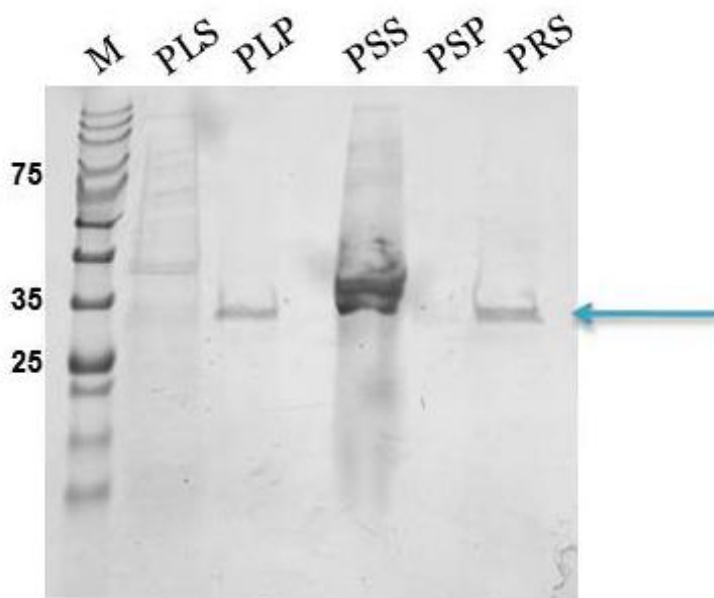


Figure 19: TbALR' post cell lysis, post pellet solubilization, and post protein renaturation. Lane 1 (M) is the marker. Molecular weights of the marker are in kDa. Lane 2 (PLS) is the soluble fraction post cell lysis. Lane 3 (PLP) is the insoluble fraction post cell lysis. Lane 4 (PSS) is the soluble fraction post denaturing and reducing. Lane 5 (PSP) is the insoluble fraction post denaturing and reducing. Lane 6 (PRS) is the solution after being renatured. PLS: Post Lysis Supernatant; PLP: Post Lysis Pellet; PSS: Post Solubilizing Supernatant; PSP: Post Solubilizing Pellet; PRS: Post Renaturing Supernatant. TbALR' is indicated by a blue arrow.

Though active protein was obtained, the procedure was not without problems. The protein would not elute using imidazole concentrations lower than 3M when bound to an Ni-IDA column. This, though not ideal, would not be an obstacle if the imidazole could be removed via dialysis. Upon dialyzing the protein, the protein always precipitated from solution within hours. Hypothesizing that the relatively rapid removal of such a high concentration of imidazole was causing the precipitation, two different methods of dialysis were attempted: only submerging the bottom corner

(approximately 0.5” – 1”) of the dialysis tubing in the dialysis buffer, and reducing the concentration of imidazole in stepwise gradients, neither of which prevented precipitation.

Hydrophobic interaction chromatography was also attempted but did not bind the protein. High concentrations (50 mM and 100 mM) of EDTA were also employed with Ni-IDA chromatography but proved unable to elute the protein as well. Even allowing these reagents additional time (overnight) to elute the protein proved futile. Incubating the renatured protein with Triton X-100, a surfactant for the recovery of membrane proteins, was also unsuccessful in aiding elution.

To investigate why this was occurring, I loaded only 4% of protein from a 1 L expression onto a Ni-IDA column and 50% of protein from a 1 L expression onto a second column. Protein bound to the first column eluted with 200 mM to 500 mM imidazole. The second column, where 50% of protein from a 1 L expression was bound, would not elute prior to 3 M imidazole. After further probing, it was discovered that no greater than 9 mg of *TbALR*' can be bound to 3 mL of Ni-IDA resin for elution with moderate imidazole concentrations. This corresponds to 60 mL of renatured protein. The total volume of renatured protein I needed to load following this protocol was around 300 milliliters. Doing this via gravity flow took several hours and was too time-consuming for efficiency. Doing this via peristaltic pump proved disastrous. The protein solution would only bind to the top of the resin in the column and caused failure in the seals and column leakage.

Though precipitation does occur, the portion of the protein that remains soluble seems to remain stable as no further precipitation occurs. When concentrating this portion of protein with either PEG or via Centricon®, the protein was also prone to

precipitation. The protein seems to aggregate irreversibly on the Centricon® filter. Aggregates of protein from any of the aforementioned procedures are only able to be solubilized thorough denaturation and reduction, which is not ideal and also does not solve the issues of precipitation. Addition of 20% glycerol to the protein solution before concentration did prevent most of the aggregation.

Attempts to refold the protein after column elution were also attempted with both inclusion body purification and purification under denaturing and reducing conditions using the buffer 50 mM Tris containing 5 M Guanidine Hydrochloride, 1 mM PMSF, 0.1 mg/mL lysozyme, 1 μ M leupeptin, and 10 mM β -Mercaptoethanol, pH 7.5. Renaturing using 7x the total volume of protein made concentration via Centricon® impossible due to the large volume. Concentration using PEG took days. Refolding via dialysis proved mildly successful at preventing aggregation as long as 20% glycerol was present in the dialysis tubing and the buffer as well. Aggregation was still observed but to a lesser extent. The drawback to this was using copious amounts of glycerol. Due to the aggregation, low protein yield was also an obstacle.

TbALR' (purified via denaturing and reducing conditions) shows modest sulfhydryl oxidase activity toward the model substrate, DTT, with k_{cat} and K_m values of 165.1/min and 2.3 mM, respectively (Figure 20). Kinetic parameters of *TbALR'* compare closely, albeit a higher K_m , to the kinetic parameters of the protein obtained by Dr. Daithankar previously, as well as to the parameters obtained through my earlier inclusion body method (data not shown).

TbALR' purified via denaturing and reducing conditions lacks the purity that inclusion body purification provided. As such, the lower molecular weight band shown previously to be a fragment of *TbALR'* was still present. I sent that to Dr.

Gannon again for analysis. Five peptides were identified as “good scores.” The first peptide in sequence was IPGESPTPR. The last peptide in sequence was NSAGDGV DAGASEK. Since the *Tb*ALR’ fragment co-purifies on an Ni-IDA column with the full length *Tb*ALR’, it can be assumed that the truncated form also contains the 6X His Tag. Since the tag is located on the N-terminus of the protein, it is also safe to assume that the truncation occurs near the C-terminus. Since the NSAGDGV DAGASEK is seen, the truncation must occur after that in this region of *Tb*ALR’:

KWWRWGNSTSSSTTATIATPSAAEPAEDVEASVTSILSKLRACMVYCPDDKKSSA. This fragment is around 6 kDa, which is around the difference between the full length *Tb*ALR’ and the truncated form, so it is possible that the protein is cleaved here prematurely.

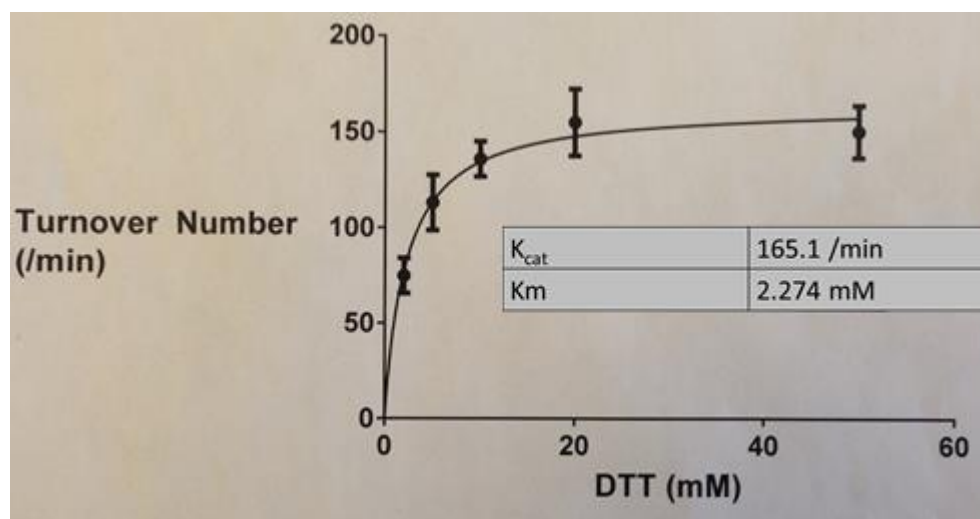


Figure 20: Michaelis-Menten parameters for *Tb*ALR’ using DTT as a substrate in an oxygen electrode assay. The buffer used was 50 mM Tris containing 1 mM EDTA and 20% glycerol, pH 8.5.

6.2 Circumventing Trypanosomal ALR's Aggregation through Generation of Fusion Proteins

In an effort to circumvent the propensity of *TbALR'* to aggregate, an effort to fuse it to a well-behaved and well-folded partner protein was initiated. One fusion protein employed the thioredoxin (Trx) domain from *E. coli*, and a second fusion protein used a maltose-binding protein from *E. coli*. Multiple attempts failed to effect ligation of the maltose-binding protein DNA sequence into the pET28a vector encoding *TbALR'*. In contrast, the thioredoxin fusion attempt was successful. The Trx: *TbALR'* mutant contained an N-terminal 6X His Tag, followed by the thioredoxin domain and a TEV protease cleavage site (ENLYFQ) (Figure 21).

Expression and purification trials were performed under various conditions. The protocol resulting in the most active protein involved expression in BL21*DE3 cells at 37 °C until an OD₆₀₀ of 0.8 was achieved, followed by 1 mM IPTG induction and 24 hours of further expression at 15 °C. Cells were harvested, resuspended in 50 mM Tris containing 1 mM PMSF and 0.1 mg/mL lysozyme at pH 8.5, and lysed via French press (2x) and sonication (5x, 30s). Cells were purified via Ni-IDA column chromatography using increasing concentrations of imidazole as the elution reagent. Expression and purification gels are shown below (Figures 22 and 23, respectively).

```

agtagtaggttgaggccgttgagcaccgcccgcgcaaggaatggtgcatgcaaggagatggcgcccaacagtccc
ccggccacggggcctgccaccatacccacgcccgaacaagcgctcatgagcccgaagtggcgagcccgatcttcc
ccatcggtgatgtcggcgatataggcggcagcaaccgcacctgtggcgccggtgatgcccggccacgatgctccg
gcgtagaggatcgagatctcgatcccgcgaaatLaatacgaactcactataggggaattgtgagcggataacaatt
cccctctagaaataattttgtttaactttaagaaggagatataccatggGTCATCACCATCATCACCATAGCGAT
AAAATTATTCACCTGACTGACGACAGTTTTGACACGGATGTACTCAAAGCGGACGGGGCGATCCTCGTCGATTTCT
TGGGCAGAGTGGTGCCTGCCGTCGAAAATGATCGCCCCGATTCTGGATGAAATCGCTGACGAATATCAGGGCAAA
CTGACCGTTGCAAACTGAACATCGATCAAAACCTGGCACTGCGCCGAAATATGGCATCCGTGGTATCCCGACT
CTGCTGCTGTTCAAAAACGGTGAAGTGGCGGCAACCAAAAGTGGGTGCACTGTCTAAAGGTCAGTTGAAAGAGTTC
CTCGACGCTAACCTGGCCGAAAACCTGTATTTTCAGTCCatgTCTAAACAGGAGCCGCTGCAGAAGATTCGGGGT
GAGTGTCCGACGCCGCTGAAGTGGGTAAAGCAGGCTGGATTATCCTGCACCTCTGCTGCCGCTGTGTTTCCGTAC
AACCTACCCCGACCCAACAGGAGGCATTCCGCAACTTTCTGCACGGCTGGTCCCACGCGTATGCTTGCAGCCAT
TGTGCATACCACATGCGTTCGTTACTTTCACCAGAATCCACCGGTCGTACCGGATAAGCTGGCACTGAACCGTTAT
CTGTGTGAATTTACAAACGCTGTAATGAGCGTGTGGTAACAAGATCTATGATTGTGACCCGATGAATGTTCTG
CGCCGTTGGCACCCAACGTTTCCAGATATGGAGGATCAACCTACCATCGAGGAACAGGTGAAGTCTCTGGAACTG
AAGGAAAAGAATGAGACCCCGCAAGGCGTTTCTGATCGTTGGCGTCAGCAGAACTCTTCCGCGTCTCCAGATGGT
AACGTTGGTCGTTGGTCTGTGGGTGACGCGCGTTGGACCGATAACCACTAGCGAGTCTCGTCTACTAATGTCGGT
GAGATCTCTGCGGGTTGGGGTACCCTGGTGAGAAGATGAAACAACGTAATTCTGCGGGTGACGGTGTCTCTGAT
GCGGGTGCAGCGAAAAGAAGTGGTGGCGTTGGGGTAACTCCACTTCTTCTTCCACTACCGCAACCATCGCAACC
CCTTCTGCAGCTGAACCTGCCGAGGATGTTGAGGCTAGCGTTACCTCTATCCTGTCTAAACTGCGTGCTTGCATG
GTTTACTGCCCTGATGATAAGAAATCTTCTGCGTGAagatccggaattcgagctccgtcgacaagcttgccggcgg

```

Figure 21: Nucleic acid sequence of Trx: TbALR fusion protein. The 6X His Tag is in green. The thioredoxin domain is in magenta. The TEV protease cleavage site is in lilac. TbALR is in cyan. The cysteines of TbALR are highlighted in yellow. The C14 position (mutated to a serine in experiments) is highlighted in magenta.

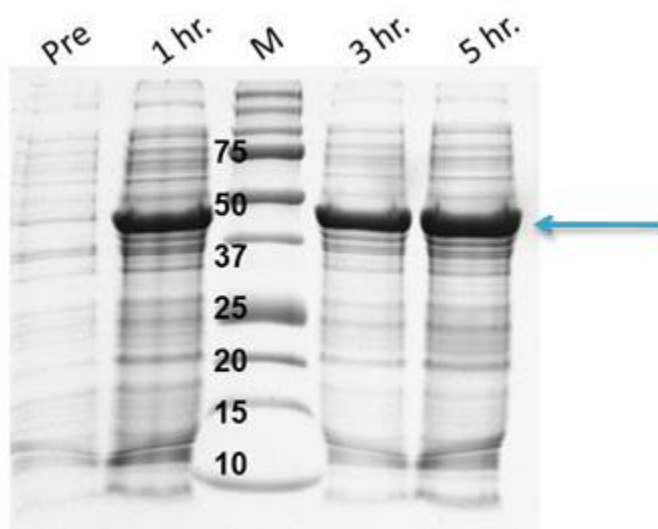


Figure 22: Expression gel of Trx: TbALR'. IPTG induction, BL21*DE3 cells, 37 °C/ 15 °C. Lane 1 is the pre-induced sample. Lanes 2, 4, and 5 are 1, 3, and 5 hours post induction, respectively. Lane 3 (M) is the marker. Molecular weights of the marker are in kDa. Trx: TbALR' is indicated by a blue arrow.

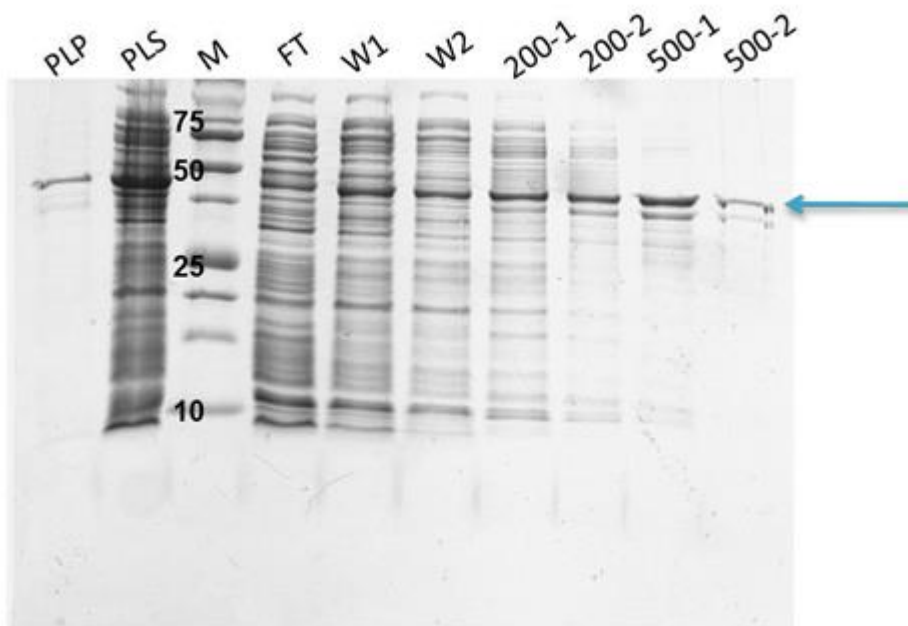


Figure 23: IMAC purification gel of Trx: TbALR' using an Ni-IDA column. Lane 1 (PLP) is the post-lysis pellet. Lane 2 (PLS) is the post lysis supernatant. Lane 3 (M) is the marker. Molecular weights of the marker are in kDa. Lane 4 (FT) is the flow through. Lanes 5 (W1) and 6 (W2) are buffer washes. Lanes 7-10 are elution fractions with 200 and 500 mM imidazole concentrations. PLP: Post Lysis Pellet; PLS: Post Lysis Supernatant; FT: Flow Through; W: Wash. Trx: TbALR' is indicated by a blue arrow.

Several attempts were made to separate the protein from thioredoxin and TEV protease upon successful cleavage (Figure 24). Immobilized metal affinity chromatography (IMAC) via Ni-IDA column was attempted first. The TEV protease and the thioredoxin domain after cleavage are both preceded by a 6X His Tag. Upon incubation with Ni-IDA resin, *TbALR'* should flow through, while TEV protease and the thioredoxin domain should bind to the resin. This was not the case. After various attempts, nothing bound to the resin. All three proteins were found in the flow through (Figure 24).

Size exclusion was employed next in an effort to first remove the small thioredoxin domain (13.4 kDa) from TEV protease (28 kDa) and *TbALR'* (30.5 kDa). This was successful (Figure 25). In an effort to then separate the TEV protease (pI of 8.3) from *TbALR'* (pI of 6.7), ion exchange chromatography was attempted as an immediate, second purification step. Poising the pH at 8 would allow *TbALR'* to bind to a negatively charged column as the protein would be positively charged. TEV protease should flow through due to its neutral charge. At pH 7, TEV protease should bind to a positively charged column, as it would be negatively charged, whereas *TbALR'* should be present in the flow through due to its neutral charge. Experiments were carried out in 20 mM Tris containing 1 mM EDTA at room temperature. Bound protein was eluted using increasing concentrations of NaCl. Both attempts failed to separate TEV protease and *TbALR'*; they both eluted at pH 8 and were also present in the flow through at pH 7 (Figure 25).

In a final attempt to separate TEV protease from *TbALR'*, hydrophobic interaction chromatography using a butyl sepharose column and a maximum of 30% ammonium sulfate was employed. Experiments were carried out in 20 mM Tris containing 1 mM EDTA at room temperature. Using both a step-wise gradient and a linear gradient of decreasing ammonium sulfate concentration did not result in protein separation. TEV protease and *TbALR'* still eluted together (data not shown). Though the reason why TEV protease and *TbALR'* could not be separated remain unknown, an interaction between the two is likely responsible.

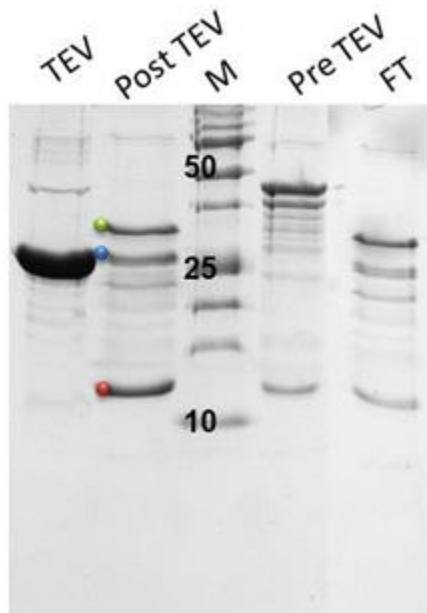


Figure 24: TEV Protease and Trx: TbALR' separation attempt via IMAC using an Ni-IDA column. Lane 1 (TEV) is TEV protease alone. Lane 2 (Post TEV) is Trx: TbALR' post incubation with TEV protease. Lane 3 (M) is the marker. Molecular weights of the marker are in kDa. Lane 4 (Pre TEV) is Trx: TbALR' before incubation with TEV protease. Lane 5 (FT) is the flow through. FT: Flow Through. Trx: TbALR' is indicated by a green dot. TEV protease is indicated by a blue dot. Thioredoxin is indicated by a red dot.

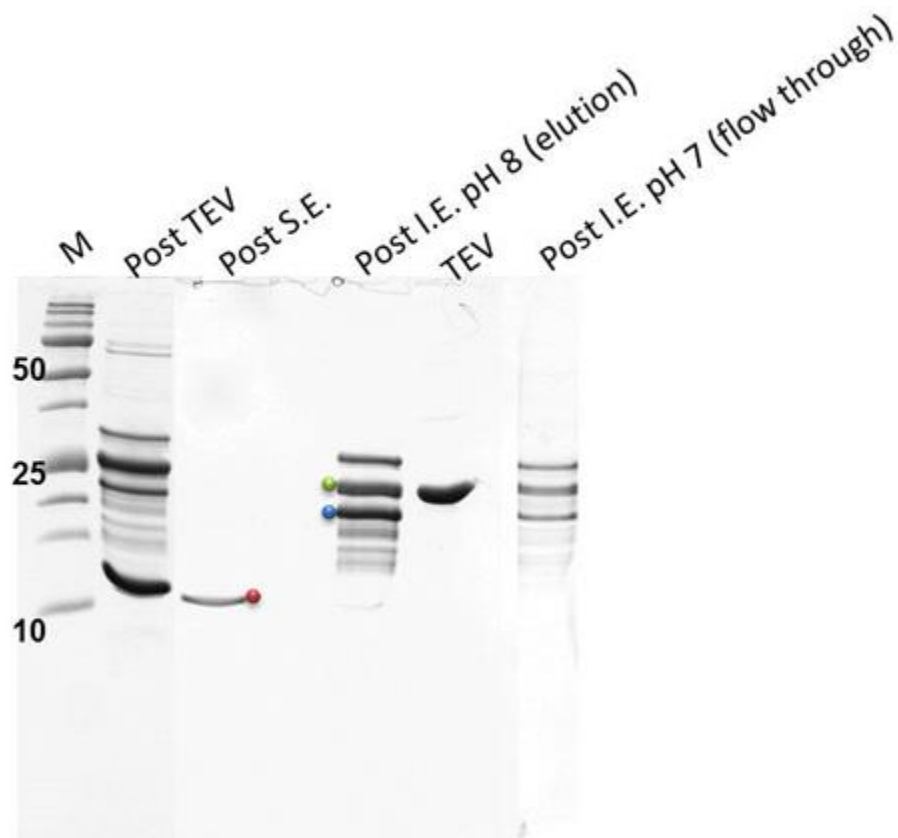


Figure 25: TEV Protease and Trx: TbALR' separation attempt via size exclusion chromatography and ion exchange chromatography. Lane 1 (M) is the marker. Molecular weights of the marker are in kDa. Lane 2 (Post TEV) is Trx: TbALR' post incubation with TEV protease. Lane 3 (Post S.E.) is Trx: TbALR' after size exclusion chromatography was performed. Lane 4 (Post I.E. pH 8) is Trx: TbALR' after anion exchange chromatography was performed. Lane 5 (TEV) is TEV protease alone. Lane 6 (Post I.E. pH 7) is Trx: TbALR' after cation exchange chromatography was performed. S.E.: Size Exclusion; I.E.: Ion Exchange. Trx: TbALR' is indicated by a green dot. TEV protease is indicated by a blue dot. Thioredoxin is indicated by a red dot.

Trx: *Tb*ALR' shows modest sulfhydryl oxidase activity toward the model substrate, DTT, with k_{cat} and K_m values of 261.6/min and 4.5 mM, respectively (Figure 26).

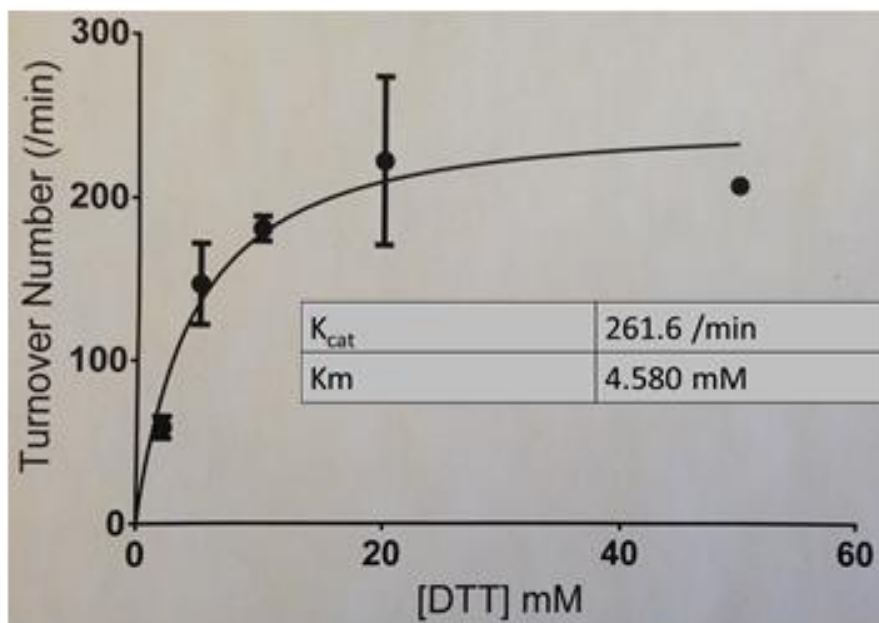


Figure 26: Michaelis-Menten parameters for Trx: *Tb*ALR' using DTT as a substrate in an oxygen electrode assay. The buffer used was 50 mM Tris containing 1 mM EDTA and 20% glycerol, pH 8.5.

6.3 Investigation of Arsenical Inhibition by Trypanosomal ALR

Paul Ehrlich, a German scientist who lived from 1854-1915, treated syphilis in humans with arsphenamine. It was the most prescribed drug in the world and was the most effective against syphilis until the emergence of penicillin. Ehrlich also treated trypanosomiasis in guinea pigs with another arsenic drug, arsenophenylglycine. He

coined the term “magic bullet,” referring to a compound that would only kill a targeted organism (e.g. trypanosomes) (58).

Previously in the lab, Dr. Daithankar showed that *Tb*ALR' is inhibited by the arsenical, succinylamidophenyl arsenoxide (PSAO) and short form human ALR is not. This is an interesting and exciting observation when remembering Ehrlich's “magic bullet” in guinea pigs. Perhaps the arsenophenylglycine was targeting and inhibiting the ALR in the guinea pig trypanosomes, leading to the death of the parasites. Arsenicals bind to free thiols in the reaction shown in Figure 27. Thiols of a sulfhydryl oxidase bound by an arsenical would then be unable to take part in the transfer of electrons necessary to complete catalysis, rendering the enzyme inactive.

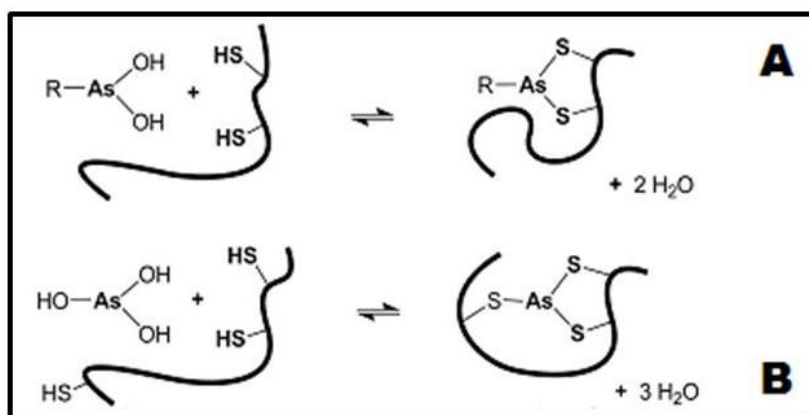


Figure 27: Coordination of thiols. Panel A shows alkyl- or aryl- arsenicals. Panel B depicts arsonous acid.

To probe this observation further, I performed an oxygen electrode assay with three separate sulfhydryl oxidases: trypanosomal ALR (*Tb*ALR'), short form human ALR (HsALR-sf), and long form human ALR (HsALR-lf)(5 μ M). Tris hydroxypropyl

phosphine (THP; 5 mM) was used as the model substrate. Thiol substrates were avoided as they would compete with the enzyme for the arsenical reagent. Superoxide dismutase (SOD; 80 U/mL) was present to eliminate artifactual phosphine-driven consumption of oxygen in the presence of the superoxide anion. PSAO in increasing concentrations (5 μ M, 10 μ M, 15 μ M, 45 μ M) was used. The assay was carried out with a total volume of 3 mL in 50 mM KPi buffer at pH 7.5 and 25 °C. Surprisingly and disappointingly, all of the enzymes were inactivated by the inhibitor. The inhibition was also reversible upon the addition of 5 mM DTT. Though *TbALR'* was inactivated more quickly, the fact that the inhibition is not unique to trypanosomal ALR as originally believed halted pursuit of this further.

Using an arsenic column designed and synthesized by current lab member, Aparna Sapra (Figure 28), *Crithidia fasciculata* lysate was used to probe for any proteins present in the organism that may be sensitive to arsenic. *Crithidia fasciculata* still belong to the Trypanosomatida order but maintain a different Genus and Species. They do not infect humans and are therefore safer for experimentation.

The *Crithidia fasciculata* cell pellet was resuspended in 10 mL of 50mM KPi containing 300mM NaCl and 1mM EDTA buffer, pH 7.5. One milliliter of the lysate was incubated with 0.5 mL arsenic resin for 2 hours in the presence of 1 mM tris(2-carboxyethyl)phosphine (TCEP). One milliliter of the lysate was incubated with 0.5 mL arsenic resin for 2 hours without TCEP. The flow through was collected, the columns were washed with buffer, and bound proteins were eluted with increasing concentrations of two reductants, β -Mercaptoethanol and dithiothreitol (Figure 29). The bands on the gel were not analyzed further as they were too numerous to be separated or identified.

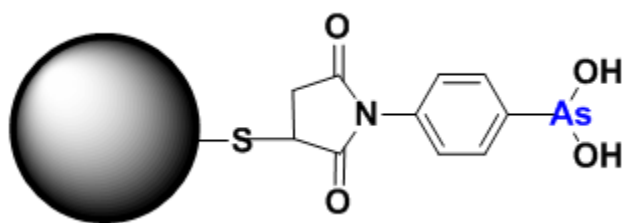


Figure 28: Representative bead of the arsenic resin designed and synthesized by Aparna Sapra.

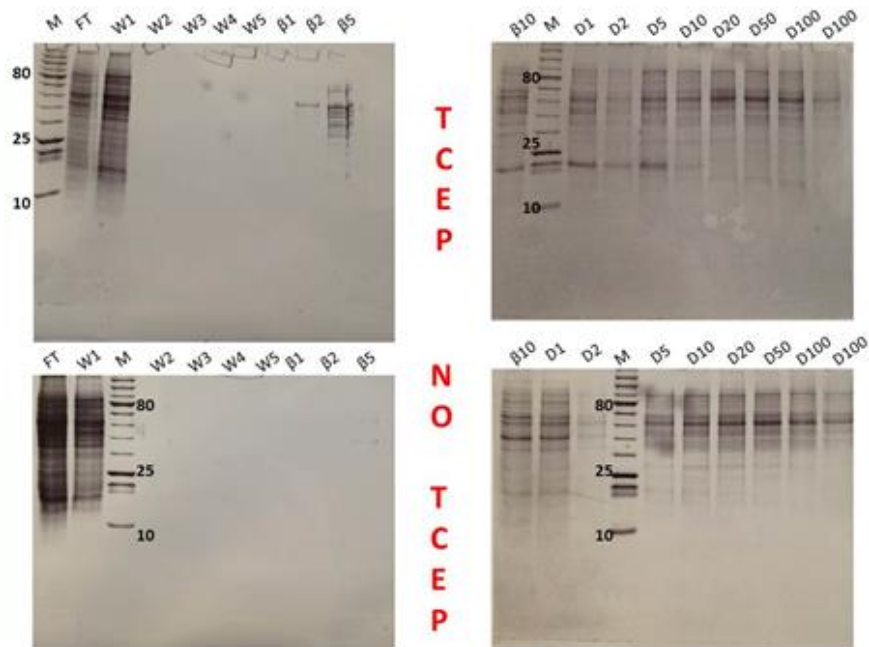


Figure 29: *Crithidia fasciculata* lysate incubated in the presence or absence of TCEP with arsenic resin. M: Marker; FT: Flow Through; W: Wash; β : β -Mercaptoethanol; D: Dithiothreitol. Molecular weights of the marker are in kDa.

6.4 Side Projects with Trypanosomal ALR

Efforts were initiated toward solving the crystal structure of both *TbALR'* and the Trx: *TbALR'* fusion protein using the Hampton Research Crystal Screen (HR2-110). *TbALR'* was attempted at 25 °C. The fusion protein was attempted at both 4 °C and 25 °C. No crystals were observed. Two double mutants of *TbALR'*, with cysteines at positions 63 and 261 mutated to alanines and serines were also created. These mutants were designed in an effort to obtain crystal structures with trapped disulfides, but were not attempted due to lack of crystallization in the other constructs. Attempts to identify partner proteins for *TbALR'* using Crithidial extracts via a pull down assay were initiated but halted due to lack of access to mass spectroscopy analysis facilities.

REFERENCES

1. Schulman, S., Wang, B., Li, W., & Rapoport, T. A. (2010). Vitamin K epoxide reductase prefers ER membrane-anchored thioredoxin-like redox partners. *Proceedings of the National Academy of Sciences of the United States of America*, *107*(34), 15027–32. doi:10.1073/pnas.1009972107
2. Sevier, C. S. (2010). New insights into oxidative folding. *The Journal of Cell Biology*, *188*(6), 757–8. doi:10.1083/jcb.201002114
3. Tavender, T. J., Springate, J. J., & Bulleid, N. J. (2010). Recycling of peroxiredoxin IV provides a novel pathway for disulphide formation in the endoplasmic reticulum. *The EMBO Journal*, *29*(24), 4185–97. doi:10.1038/emboj.2010.273
4. Thorpe, C., & Coppock, D. L. (2007). Generating disulfides in multicellular organisms: emerging roles for a new flavoprotein family. *The Journal of Biological Chemistry*, *282*(19), 13929–33. doi:10.1074/jbc.R600037200
5. Thorpe, C. (2013). Flavoproteins in oxidative protein folding. In R. Hille, S. Miller & B. Palfey (Eds.), *Handbook of flavoproteins: Volume 1 Oxidases, Dehydrogenases, and Related Systems* (1 ed., Vol. 1, pp. 249-269). Boston, MA: Walter De Gruyter
6. Zito, E., Melo, E. P., Yang, Y., Wahlander, Å., Neubert, T. A., & Ron, D. (2010). Oxidative protein folding by an endoplasmic reticulum-localized peroxiredoxin. *Molecular Cell*, *40*(5), 787–97. doi:10.1016/j.molcel.2010.11.010
7. Riemer, J., Fischer, M., & Herrmann, J. M. (2011). Oxidation-driven protein import into mitochondria: Insights and blind spots. *Biochimica et Biophysica Acta*, *1808*(3), 981–9. doi:10.1016/j.bbamem.2010.06.003
8. Ostrowski, M. C., & Kistler, W. S. (1980). Properties of a flavoprotein sulfhydryl oxidase from rat seminal vesicle secretion. *Biochemistry*, *19*(12), 2639–45. Retrieved from <http://www.ncbi.nlm.nih.gov/pubmed/7397095>

9. Benayoun, B., Esnard-Fève, A., Castella, S., Courty, Y., & Esnard, F. (2001). Rat seminal vesicle FAD-dependent sulfhydryl oxidase. Biochemical characterization and molecular cloning of a member of the new sulfhydryl oxidase/quiescin Q6 gene family. *The Journal of Biological Chemistry*, 276(17), 13830–7. doi:10.1074/jbc.M010933200
10. Hooper, K. L., Glynn, N. M., Burnside, J., Coppock, D. L., & Thorpe, C. (1999). Homology between Egg White Sulfhydryl Oxidase and Quiescin Q6 Defines a New Class of Flavin-linked Sulfhydryl Oxidases. *J. Biol. Chem.*, 274(45), 31759–31762. Retrieved from <http://www.jbc.org/content/274/45/31759.long>
11. Kodali, V. K., & Thorpe, C. (2010a). Oxidative protein folding and the Quiescin-sulfhydryl oxidase family of flavoproteins. *Antioxidants & Redox Signaling*, 13(8), 1217–30. doi:10.1089/ars.2010.3098
12. Hatahet, F., & Ruddock, L. W. (2009). Protein disulfide isomerase: a critical evaluation of its function in disulfide bond formation. *Antioxidants & Redox Signaling*, 11(11), 2807–50. doi:10.1089/ARS.2009.2466
13. Wilkinson, B., & Gilbert, H. F. (2004). Protein disulfide isomerase. *Biochimica et Biophysica Acta*, 1699(1-2), 35–44. doi:10.1016/j.bbapap.2004.02.017
14. Farrell, S. R., & Thorpe, C. (2005). Augmenter of liver regeneration: a flavin-dependent sulfhydryl oxidase with cytochrome c reductase activity. *Biochemistry*, 44(5), 1532–41. doi:10.1021/bi0479555
15. Thorpe, C., Hooper, K. L., Raje, S., Glynn, N. M., Burnside, J., Turi, G. K., & Coppock, D. L. (2002). Sulfhydryl oxidases: emerging catalysts of protein disulfide bond formation in eukaryotes. *Archives of Biochemistry and Biophysics*, 405(1), 1–12. Retrieved from <http://www.ncbi.nlm.nih.gov/pubmed/12176051>
16. Stein, G., & Lisowsky, T. (1998). Functional comparison of the yeast scERV1 and scERV2 genes. *Yeast (Chichester, England)*, 14(2), 171–80. doi:10.1002/(SICI)1097-0061(19980130)14:2<171::AID-YEA209>3.0.CO;2-U
17. Coddling, J. a, Israel, B. a, & Thorpe, C. (2012). Protein substrate discrimination in the quiescin sulfhydryl oxidase (QSOX) family. *Biochemistry*, 51(20), 4226–35. doi:10.1021/bi300394w

18. Hooper, K. L., Sheasley, S. L., Gilbert, H. F., & Thorpe, C. (1999). Sulfhydryl oxidase from egg white. A facile catalyst for disulfide bond formation in proteins and peptides. *The Journal of Biological Chemistry*, 274(32), 22147–50. Retrieved from <http://www.ncbi.nlm.nih.gov/pubmed/10428777>
19. Alon, A., Heckler, E. J., Thorpe, C., & Fass, D. (2010). QSOX contains a pseudo-dimer of functional and degenerate sulfhydryl oxidase domains. *FEBS Letters*, 584(8), 1521–5. doi:10.1016/j.febslet.2010.03.001
20. Heckler, E. J., Alon, A., Fass, D., & Thorpe, C. (2008). Human quiescin-sulfhydryl oxidase, QSOX1: probing internal redox steps by mutagenesis. *Biochemistry*, 47(17), 4955–63. doi:10.1021/bi702522q
21. Kodali, V. K., & Thorpe, C. (2010b). Quiescin sulfhydryl oxidase from *Trypanosoma brucei*: catalytic activity and mechanism of a QSOX family member with a single thioredoxin domain. *Biochemistry*, 49(9), 2075–85. doi:10.1021/bi902222s
22. Heckler, E. J., Rancy, P. C., Kodali, V. K., & Thorpe, C. (2008). Generating disulfides with the Quiescin-sulfhydryl oxidases. *Biochimica et Biophysica Acta*, 1783(4), 567–77. doi:10.1016/j.bbamcr.2007.10.002
23. Raje, S., & Thorpe, C. (2003). Inter-domain redox communication in flavoenzymes of the quiescin/sulfhydryl oxidase family: role of a thioredoxin domain in disulfide bond formation. *Biochemistry*, 42(15), 4560–8. doi:10.1021/bi030003z
24. Jaje, J., Wolcott, H. N., Fadugba, O., Cripps, D., Yang, A. J., Mather, I. H., & Thorpe, C. (2007). A flavin-dependent sulfhydryl oxidase in bovine milk. *Biochemistry*, 46(45), 13031–40. doi:10.1021/bi7016975
25. Raje, S., Glynn, N. M., & Thorpe, C. (2002). A continuous fluorescence assay for sulfhydryl oxidase. *Analytical Biochemistry*, 307(2), 266–272. doi:10.1016/S0003-2697(02)00050-7
26. Zanata, S. M., Luvizon, A. C., Batista, D. F., Ikegami, C. M., Pedrosa, F. O., Souza, E. M., ... Nakao, L. S. (2005). High levels of active quiescin Q6 sulfhydryl oxidase (QSOX) are selectively present in fetal serum. *Redox Report : Communications in Free Radical Research*, 10(6), 319–23. doi:10.1179/135100005X83699

27. Mairet-Coello, G., Tury, A., Esnard-Feve, A., Fellmann, D., Risold, P.-Y., & Griffond, B. (2004). FAD-linked sulfhydryl oxidase QSOX: topographic, cellular, and subcellular immunolocalization in adult rat central nervous system. *The Journal of Comparative Neurology*, *473*(3), 334–63. doi:10.1002/cne.20126
28. Martin, D. B., Gifford, D. R., Wright, M. E., Keller, A., Yi, E., Goodlett, D. R., ... Nelson, P. S. (2004). Quantitative proteomic analysis of proteins released by neoplastic prostate epithelium. *Cancer Research*, *64*(1), 347–55. Retrieved from <http://www.ncbi.nlm.nih.gov/pubmed/14729644>
29. Katchman, B. A., Antwi, K., Hostetter, G., Demeure, M. J., Watanabe, A., Decker, G. A., ... Lake, D. F. (2011). Quiescin sulfhydryl oxidase 1 promotes invasion of pancreatic tumor cells mediated by matrix metalloproteinases. *Molecular Cancer Research : MCR*, *9*(12), 1621–31. doi:10.1158/1541-7786.MCR-11-0018
30. Guo, P.-C., Ma, J.-D., Jiang, Y.-L., Wang, S.-J., Bao, Z.-Z., Yu, X.-J., ... Zhou, C.-Z. (2012). Structure of yeast sulfhydryl oxidase Erv1 reveals electron transfer of the disulfide relay system in the mitochondrial intermembrane space. *Journal of Biological Chemistry*. doi:10.1074/jbc.M112.394759
31. Fass, D. (2008). The Erv family of sulfhydryl oxidases. *Biochimica et Biophysica Acta*, *1783*(4), 557–66. doi:10.1016/j.bbamcr.2007.11.009
32. Gross, E., Sevier, C. S., Vala, A., Kaiser, C. A., & Fass, D. (2002). A new FAD-binding fold and intersubunit disulfide shuttle in the thiol oxidase Erv2p. *Nature Structural Biology*, *9*(1), 61–7. doi:10.1038/nsb740
33. Hakim, M., & Fass, D. (2010). Cytosolic disulfide bond formation in cells infected with large nucleocytoplasmic DNA viruses. *Antioxidants & Redox Signaling*, *13*(8), 1261–71. doi:10.1089/ars.2010.3128
34. Daithankar, V. N., Wang, W., Trujillo, J. R., & Thorpe, C. (2012). Flavin-linked Erv-family sulfhydryl oxidases release superoxide anion during catalytic turnover. *Biochemistry*, *51*(1), 265–72. doi:10.1021/bi201672h
35. Chacinska, A., Koehler, C. M., Milenkovic, D., Lithgow, T., & Pfanner, N. (2009). Importing mitochondrial proteins: machineries and mechanisms. *Cell*, *138*(4), 628–44. doi:10.1016/j.cell.2009.08.005

36. Deponte, M., & Hell, K. (2009). Disulphide bond formation in the intermembrane space of mitochondria. *Journal of Biochemistry*, 146(5), 599–608. doi:10.1093/jb/mvp133
37. Endo, T., Yamano, K., & Kawano, S. (2010). Structural basis for the disulfide relay system in the mitochondrial intermembrane space. *Antioxidants & Redox Signaling*, 13(9), 1359–73. doi:10.1089/ars.2010.3099
38. Herrmann, J. M., & Riemer, J. (2012). Mitochondrial disulfide relay: redox-regulated protein import into the intermembrane space. *The Journal of Biological Chemistry*, 287(7), 4426–33. doi:10.1074/jbc.R111.270678
39. Wu, C.-K., Dailey, T. A., Dailey, H. A., Wang, B.-C., & Rose, J. P. (2003). The crystal structure of augments of liver regeneration: A mammalian FAD-dependent sulfhydryl oxidase. *Protein Science : A Publication of the Protein Society*, 12(5), 1109–18. doi:10.1110/ps.0238103
40. Daithankar, V. N., Schaefer, S. A., Dong, M., Bahnson, B. J., & Thorpe, C. (2010). Structure of the human sulfhydryl oxidase augments of liver regeneration and characterization of a human mutation causing an autosomal recessive myopathy. *Biochemistry*, 49(31), 6737–45. doi:10.1021/bi100912m
41. Hagiya, M., Francavilla, A., Polimeno, L., Ihara, I., Sakai, H., Seki, T., ... Starzl, T. E. (1994). Cloning and sequence analysis of the rat augments of liver regeneration (ALR) gene: expression of biologically active recombinant ALR and demonstration of tissue distribution. *Proceedings of the National Academy of Sciences of the United States of America*, 91(17), 8142–6. Retrieved from <http://www.pubmedcentral.nih.gov/articlerender.fcgi?artid=44561&tool=pmcentrez&rendertype=abstract>
42. Sankar, U., & Means, A. R. (2011). Gfer is a critical regulator of HSC proliferation. *Cell Cycle (Georgetown, Tex.)*, 10(14), 2263–8. Retrieved from <http://www.pubmedcentral.nih.gov/articlerender.fcgi?artid=3230525&tool=pmcentrez&rendertype=abstract>
43. Di Fonzo, A., Ronchi, D., Lodi, T., Fassone, E., Tigano, M., Lamperti, C., ... Comi, G. P. (2009). The mitochondrial disulfide relay system protein GFER is mutated in autosomal-recessive myopathy with cataract and combined respiratory-chain deficiency. *American Journal of Human Genetics*, 84(5), 594–604. doi:10.1016/j.ajhg.2009.04.004

44. Daithankar, V. N., Farrell, S. R., & Thorpe, C. (2009). Augmenter of liver regeneration: substrate specificity of a flavin-dependent oxidoreductase from the mitochondrial intermembrane space. *Biochemistry*, 48(22), 4828–37. doi:10.1021/bi900347v
45. Hunt, R. (2010). *Eukaryotic cells with a different way of doing things*. Retrieved from <http://pathmicro.med.sc.edu/lecture/trypanosomiasis.htm>
46. Schneider, A., Bursac, D., & Lithgow, T. (2008). The direct route: a simplified pathway for protein import into the mitochondrion of trypanosomes. *Trends in Cell Biology*, 18(1), 12–8. doi:10.1016/j.tcb.2007.09.009
47. World Health Organization. (2012). *Human African Trypanosomiasis*. Retrieved from www.who.int/trypanosomiasis_african/en/
48. Centers for Disease Control and Prevention. (2010). *African Trypanosomiasis*. Retrieved from www.cdc.gov/parasites/sleepingsickness/
49. Bacchi, C. J. (2009). Chemotherapy of human african trypanosomiasis. *Interdisciplinary Perspectives on Infectious Diseases*, 2009, 195040. doi:10.1155/2009/195040
50. Pays, E., Lheureux, M., & Steinert, M. (1981). The expression-linked copy of a surface antigen gene in *Trypanosoma* is probably the one transcribed. *Nature*, 292(5820), 265–7. Retrieved from <http://www.ncbi.nlm.nih.gov/pubmed/7254319>
51. Opperdoes, F. (1997). *Structure of trypanosome VSG*. Retrieved from www.icp.ucl.ac.be/~opperd/parasites/vsg.htm
52. Barry D, Carrington M. (2012). Antigenic variation and the variant surface glycoprotein (VSG). Retrieved from leishman.cent.gla.ac.uk/kook_about.html
53. Mehlert, A., Bond, C. S., & Ferguson, M. a J. (2002). The glycoforms of a *Trypanosoma brucei* variant surface glycoprotein and molecular modeling of a glycosylated surface coat. *Glycobiology*, 12(10), 607–12. Retrieved from <http://www.ncbi.nlm.nih.gov/pubmed/12244073>
54. ClustalW2. (2012). Retrieved from www.ebi.ac.uk/Tools/msa/clustalw2/

55. Allen, J. W. a, Ferguson, S. J., & Ginger, M. L. (2008). Distinctive biochemistry in the trypanosome mitochondrial intermembrane space suggests a model for stepwise evolution of the MIA pathway for import of cysteine-rich proteins. *FEBS Letters*, 582(19), 2817–25. doi:10.1016/j.febslet.2008.07.015
56. Basu, S., Leonard, J. C., Desai, N., Mavridou, D. a I., Tang, K. H., Goddard, A. D., ... Allen, J. W. a. (2013). Divergence of Erv1-associated mitochondrial import and export pathways in trypanosomes and anaerobic protists. *Eukaryotic Cell*, 12(2), 343–55. doi:10.1128/EC.00304-12
57. Krauth-Siegel, R. L., & Comini, M. a. (2008). Redox control in trypanosomatids, parasitic protozoa with trypanothione-based thiol metabolism. *Biochimica et Biophysica Acta*, 1780(11), 1236–48. doi:10.1016/j.bbagen.2008.03.006
58. *Paul ehrlich*. (2014). Retrieved from http://en.wikipedia.org/wiki/Paul_Ehrlich
59. Vitu, E., Bentzur, M., Lisowsky, T., Kaiser, C. a, & Fass, D. (2006). Gain of function in an ERV/ALR sulfhydryl oxidase by molecular engineering of the shuttle disulfide. *Journal of Molecular Biology*, 362(1), 89–101. doi:10.1016/j.jmb.2006.06.070

Appendix
PERMISSION LETTERS



RightsLink®

[Home](#)
[Create Account](#)
[Help](#)

ACS Publications

High quality. High impact.

Title: Augmenter of Liver Regeneration: Substrate Specificity of a Flavin-Dependent Oxidoreductase from the Mitochondrial Intermembrane Space

Author: Vidyadhar N. Daithankar, Scott R. Farrell, and Colin Thorpe

Publication: Biochemistry

Publisher: American Chemical Society

Date: Jun 1, 2009

Copyright © 2009, American Chemical Society

User ID
<input type="text"/>
Password
<input type="text"/>
<input type="checkbox"/> Enable Auto Login
<input type="button" value="LOGIN"/>
Forgot Password/User ID?
If you're a copyright.com user, you can login to RightsLink using your copyright.com credentials. Already a RightsLink user or want to learn more?

PERMISSION/LICENSE IS GRANTED FOR YOUR ORDER AT NO CHARGE

This type of permission/license, instead of the standard Terms & Conditions, is sent to you because no fee is being charged for your order. Please note the following:

- Permission is granted for your request in both print and electronic formats, and translations.
- If figures and/or tables were requested, they may be adapted or used in part.
- Please print this page for your records and send a copy of it to your publisher/graduate school.
- Appropriate credit for the requested material should be given as follows: "Reprinted (adapted) with permission from (COMPLETE REFERENCE CITATION). Copyright (YEAR) American Chemical Society." Insert appropriate information in place of the capitalized words.
- One-time permission is granted only for the use specified in your request. No additional uses are granted (such as derivative works or other editions). For any other uses, please submit a new request.

If credit is given to another source for the material you requested, permission must be obtained from that source.

[BACK](#)
[CLOSE WINDOW](#)

Copyright © 2014 [Copyright Clearance Center, Inc.](#) All Rights Reserved. [Privacy statement.](#) Comments? We would like to hear from you. E-mail us at customercare@copyright.com



RightsLink®

[Home](#)
[Create Account](#)
[Help](#)

ACS Publications

High quality. High impact.

Title: Structure of the Human Sulphydryl Oxidase Augmenter of Liver Regeneration and Characterization of a Human Mutation Causing an Autosomal Recessive Myopathy,

Author: Vidyadhar N. Daithankar, Stephanie A. Schaefer, Ming Dong, Brian J. Bahnson, and Colin Thorpe

Publication: Biochemistry

Publisher: American Chemical Society

Date: Aug 1, 2010

Copyright © 2010, American Chemical Society

User ID
Password
<input type="checkbox"/> Enable Auto Login
<input type="button" value="LOGIN"/>
Forgot Password/User ID?
If you're a copyright.com user, you can login to RightsLink using your copyright.com credentials. Already a RightsLink user or want to learn more?

PERMISSION/LICENSE IS GRANTED FOR YOUR ORDER AT NO CHARGE

This type of permission/license, instead of the standard Terms & Conditions, is sent to you because no fee is being charged for your order. Please note the following:

- Permission is granted for your request in both print and electronic formats, and translations.
- If figures and/or tables were requested, they may be adapted or used in part.
- Please print this page for your records and send a copy of it to your publisher/graduate school.
- Appropriate credit for the requested material should be given as follows: "Reprinted (adapted) with permission from (COMPLETE REFERENCE CITATION). Copyright (YEAR) American Chemical Society." Insert appropriate information in place of the capitalized words.
- One-time permission is granted only for the use specified in your request. No additional uses are granted (such as derivative works or other editions). For any other uses, please submit a new request.

If credit is given to another source for the material you requested, permission must be obtained from that source.

Copyright © 2014 [Copyright Clearance Center, Inc.](#) All Rights Reserved. [Privacy statement.](#) Comments? We would like to hear from you. E-mail us at customercare@copyright.com



RightsLink®

[Home](#)
[Create Account](#)
[Help](#)

ACS Publications

High quality. High impact.

Title: Protein Substrate Discrimination in the Quiescin Sulfhydryl Oxidase (QSOX) Family

Author: Jennifer A. Coddling, Benjamin A. Israel, and Colin Thorpe

Publication: Biochemistry

Publisher: American Chemical Society

Date: May 1, 2012

Copyright © 2012, American Chemical Society

User ID
Password
<input type="checkbox"/> Enable Auto Login
<input type="button" value="LOGIN"/>
Forgot Password/User ID?
If you're a copyright.com user, you can login to RightsLink using your copyright.com credentials. Already a RightsLink user or want to learn more?

PERMISSION/LICENSE IS GRANTED FOR YOUR ORDER AT NO CHARGE

This type of permission/license, instead of the standard Terms & Conditions, is sent to you because no fee is being charged for your order. Please note the following:

- Permission is granted for your request in both print and electronic formats, and translations.
- If figures and/or tables were requested, they may be adapted or used in part.
- Please print this page for your records and send a copy of it to your publisher/graduate school.
- Appropriate credit for the requested material should be given as follows: "Reprinted (adapted) with permission from (COMPLETE REFERENCE CITATION). Copyright (YEAR) American Chemical Society." Insert appropriate information in place of the capitalized words.
- One-time permission is granted only for the use specified in your request. No additional uses are granted (such as derivative works or other editions). For any other uses, please submit a new request.

If credit is given to another source for the material you requested, permission must be obtained from that source.

[BACK](#)
[CLOSE WINDOW](#)

Copyright © 2014 [Copyright Clearance Center, Inc.](#) All Rights Reserved. [Privacy statement.](#) Comments? We would like to hear from you. E-mail us at customercare@copyright.com



RightsLink®

[Home](#)
[Create Account](#)
[Help](#)


Title: Generating Disulfides in Multicellular Organisms: Emerging Roles for a New Flavoprotein Family

Author: Colin Thorpe, Donald L. Coppock

Publication: Journal of Biological Chemistry

Publisher: The American Society for Biochemistry and Molecular Biology

Date: May 11, 2007

Copyright © 2007, by the American Society for Biochemistry and Molecular Biology

User ID
<input type="text"/>
Password
<input type="text"/>
<input type="checkbox"/> Enable Auto Login
<input type="button" value="LOGIN"/>
Forgot Password/User ID?
If you're a copyright.com user, you can login to RightsLink using your copyright.com credentials. Already a RightsLink user or want to learn more?

Download Letter of Permission for Reuse in Thesis/Dissertation

The publisher allows article reuse in thesis or dissertations at no charge. [Click here to receive a letter of permission for this purpose.](#)

[BACK](#)
[CLOSE WINDOW](#)

Copyright © 2014 [Copyright Clearance Center, Inc.](#) All Rights Reserved. [Privacy statement.](#) Comments? We would like to hear from you. E-mail us at customercare@copyright.com



11200 Rockville Pike
Suite 302
Rockville, Maryland 20852

August 19, 2011

American Society for Biochemistry and Molecular Biology

To whom it may concern,

It is the policy of the American Society for Biochemistry and Molecular Biology to allow reuse of any material published in its journals (the *Journal of Biological Chemistry*, *Molecular & Cellular Proteomics* and the *Journal of Lipid Research*) in a thesis or dissertation at no cost and with no explicit permission needed. Please see our copyright permissions page on the journal site for more information.

Best wishes,

Sarah Crespi

[American Society for Biochemistry and Molecular Biology](#)

11200 Rockville Pike, Rockville, MD

Suite 302

240-283-6616

[JBC](#) | [MCP](#) | [JLR](#)

Tel: 240-283-6600 • Fax: 240-881-2080 • E-mail: asbmb@asbmb.org